

TECHNICAL REPORT

69-18-PR

RESPONSE OF POLYMERS TO TENSILE IMPACT.

1. AN INTEGRAL-EQUATION, SUCCESSIVE-SUBSTITUTION SOLUTION FOR USE IN DIGITAL COMPUTERS, AND ITS APPLICATION TO A LINEAR ELASTIC MODEL

by

Prescott D. Crout

Massachusetts Institute of Technology

and

Malcolm N. Pilsworth, Jr.

Harold J. Hoge

U.S. Army Natick Laboratories

July 1968

UNITED STATES ARMY
NATICK LABORATORIES
Natick, Massachusetts 01760



Pioneering Research Laboratory

This document has been approved for public release and sale;
its distribution is unlimited.

The findings in this report are not to be construed as an
official Department of the Army position unless so designated
by other authorized documents.

Citation of trade names in this report does not constitute
an official indorsement or approval of the use of such items.

Destroy this report when no longer needed. Do not return
it to the originator.

This document has been approved
for public release and sale; its
distribution is unlimited

AD _____

TECHNICAL REPORT
69-18-PR

RESPONSE OF POLYMERS TO TENSILE IMPACT.

I. AN INTEGRAL-EQUATION, SUCCESSIVE-SUBSTITUTION SOLUTION
FOR USE IN DIGITAL COMPUTERS, AND ITS APPLICATION TO
A LINEAR ELASTIC MODEL

by

Prescott D. Crout
Massachusetts Institute of Technology

and

Malcolm N. Pilsworth, Jr.
Harold J. Hoge
U. S. Army Natick Laboratories

Project Reference:
1T061102B11A-07

July 1968

Pioneering Research Laboratory
U. S. ARMY NATICK LABORATORIES
Natick, Massachusetts

FOREWORD

The results of high-speed tensile-impact experiments performed in the Pioneering Research Laboratory have in the past been analyzed by graphical methods based on the method of characteristics. The present report is the first of a series of three in which a new numerical method suitable for use in high-speed computers is described.

The division into three reports is based on the successive stages in the mathematical analysis as carried out by Professor Crout. In the present report the basic mathematical technique is presented and applied to a linear material, so that the method can be tested in a situation where the solution is already known. In the second report the method will be extended to non-linear materials, and in the third report the case of non-linear materials exhibiting time-dependent response (such as creep) will be treated.

The project reference number for this work is 1T061102B11A-07.

CONTENTS

	Page
List of Figures	v
Nomenclature	viii
Abstract	x
1. History and Scope.	1
2. Introduction.	2
3. Statement of Problem.	5
4. Partial Differential Equation Approach.	12
5. Integral Equation Approach.	21
6. Development of Approximate Methods for Solving the Integral Equation by Successive Substitution.	28
7. Preliminary Investigations.	40
8. Preliminary Calculations.	43
9. Description of the Repetitive Process when Applied to the Linear String.	51
10. Typical Results Obtained by Digital Computer, Using the New Methods.	54
Appendix A. Motion of Moving End Specified Arbitrarily.	63
Appendix B. Numerical Method when End Motion is Specified Arbitrarily.	69
References.	71

List of Figures

	<u>Page</u>
Fig. 1 String subjected to tensile impact.	5
Fig. 2 Viscoelastic model consisting of a spring paralleled by a dashpot.	7
Fig. 3 Model in which the modulus E increases with strain.	7
Fig. 4 Three-element viscoelastic model.	9
Fig. 5 Multi-element viscoelastic model.	9
Fig. 6 Infinitesimal element of impacted string.	13
Fig. 7 Functions involved in the general solution of the partial differential equation.	16
Fig. 8 Illustration showing how $s(x,t)$ may be obtained from $g(x)$.	17
Fig. 9 Views of the surface $s = s(x,t)$ showing transition lines between the plane portions of the surface. At the left is a side view in the $+x$ direction, and at the right is a top view in the $(-s)$ direction.	31
Fig. 10 Three dimensional view of the surface $s(x,t)$.	32
Fig. 11 Diagram for deriving relations satisfied by a cylindrical surface.	33
Fig. 12 Application of cylindrical-surface approximation to a transition line.	34
Fig. 13 Intersection of cylindrical surface with the x,t plane.	35
Fig. 14 Top view of the $s(x,t)$ surface with variables normalized. Values of $\partial s / \partial t$ and $\partial s / \partial x$ are shown for the various regions; the values change abruptly at the transition lines.	38
Fig. 15 Comparison between the approximate (successive substitution) solution and the exact solution, for $n = 20$ and $j = 1$ to 6 ($t = .05$ to $.25$). The approximate solution agreed exactly with the solution of the difference equations, which showed that the successive substitution process had converged.	42

Fig. 16	Convergence of s-values at two selected lattice points in the first row. Solid line, unmodified procedure; other lines, modified output taken as $\alpha \times \text{input} + \beta \times \text{unmodified output}$.	44
Fig. 17	Schematic representation of successive substitution process.	45
Fig. 18	Schematic representation of one step in modified substitution process, in which the weighting factors α and β are used.	46
Fig. 19	Convergence of s-values at two selected lattice points in the sixth row. The use of an extrapolated input is compared with the use of the values in the preceding row. Also, the effect of using weighting factors is shown.	49
Fig. 20	Lattice of points at which calculations are to be made.	52
Fig. 21	Values of s calculated by digital computer with $n = 100$. The lower curve is for $j = 75$ ($t = .75$) and the upper is for $j = 275$ ($t = 2.75$).	55
Fig. 22	Values of strain (ϵ) taken from the computer data of Fig. 21.	57
Fig. 23	Strain as obtained from digital computer calculations, for $n = 60$ with $j = 105$ ($t = 1.75$). In earlier graphs the acceleration of the impacted end of the string has occurred in zero time whereas here the acceleration is finite and constant and occurs in the interval $t = 0$ to $.5$.	60
Fig. 24	Strain calculated with $n = 100$, at $j = 50$ ($t = .5$) and $j = 150$ ($t = 1.5$). Note that in the time interval between the two curves, the oscillations in the computer solution have been greatly reduced by the successive-substitution process. Infinite initial acceleration (square wave).	62
Fig. 25	Representation of a continuous velocity function $v_0(t)$ by a series of step functions.	65

	<u>Page</u>
Fig. 26 Time derivative of the displacement due to an end velocity which is a unit step function.	66
Fig. 27 Graph showing the two factors in the integrand of s , when the displacement is given by a superposition integral.	67
Fig. 28 Graphs of functions to be used in finding $s(x,t)$.	68
Fig. 29 Velocity of moving end of string. The actual velocity is approximated by adding a finite increment to v_n at each successive row.	69

NOMENCLATURE

- A = cross-section area of unstretched sample.
 A_{ij} = first time-integral of the repetitive process, corresponding to the lattice point in the i^{th} column and the j^{th} row.
 B_{ij} = second time-integral of repetitive process.
 c = velocity of propagation of strain waves.
 E = modulus of elasticity.
 f = function representing strain wave traveling toward the right.
 g = function representing strain wave traveling toward the left, also see \bar{g} .
 \bar{g} = g/cv_0 ; the bar is dropped after the quantity is introduced.
 h = lattice spacing, L/n in the x -direction, L/cn in the t -direction (square lattice).
 I_k = input for the k^{th} step of the repetitive process.
 i = subscript indicating the column number of a lattice point.
 J_k = output of the k^{th} step of the repetitive process.
 j = subscript indicating the row number of a lattice point.
 k = $n\pi/L$, a quantity appearing in the Fourier-series solution; also, a term index in the difference-equation solution; also, a repetition index (superscript) in the repetitive process.
 L = length of unstretched sample.
 n = number of lattice-point intervals in the length L ; also, a term index in the Fourier-series solution and elsewhere.
 p = parameter that occurs in the Laplace transform.
 s = displacement of a particle of material from its unstretched position x , also see \bar{s} .
 \bar{s} = s/Lv_0 ; the bar is dropped after the quantity is introduced.

T = function of t in the Fourier-series solution.
 t = time, also see \bar{t} .
 \bar{t} = tc/L ; the bar is dropped after the quantity is introduced.
 u = $x \pm ct$.
 v = velocity of a particle of sample.
 v_0 = velocity of moving end of sample.
 X = function of x in the Fourier-series solution.
 x = distance of a particle of material from the fixed (left) end of the sample, in the unstretched state, also see \bar{x} .
 \bar{x} = x/L ; the bar is dropped after the quantity is introduced.
 α = the first of two weighting factors used to speed up convergence.
 β = the second of two weighting factors used to speed up convergence; $\alpha + \beta = 1$.
 ϵ = normal strain along axis of string, = $\partial s / \partial x$.
 ρ = density of unstretched material.
 σ = normal stress along axis of string.
 τ = time, variable of integration in superposition integral.

ABSTRACT

An integral-equation, modified successive-substitution method of solving the equation of motion of a linear elastic string is derived. The method is an extension to two independent variables of a method previously employed with only a single independent variable. The solution is proved to be correct in the linear case and is expected to be valid also for nonlinear cases and for situations in which the response of the material is time dependent. Methods of numerical approximation based on a lattice of points in the time-position plane are developed, suitable for digital-computer programming. Typical results of computer runs on linear materials are presented.

RESPONSE OF POLYMERS TO TENSILE IMPACT.

1. An Integral-Equation, Successive-Substitution Solution for Use in Digital Computers, and Its Application to a Linear Elastic Model.

1. History and Scope

The results now being reported have come from the combined efforts of several individuals and groups. Professor Prescott D. Crout, Mathematics Department, Massachusetts Institute of Technology, is responsible for the mathematical developments. Mr. Malcolm N. Pilsworth, Jr., of the Thermodynamics Group, U. S. Army Natick Laboratories, is responsible for the experimental data. The Computer Branch of the Natick Laboratories did the detailed programming and carried out the machine computations. Much of the planning of the work was done jointly by Professor Crout, Mr. Pilsworth, and Dr. Harold J. Hoge of the Thermodynamics Group.

The project has been concerned with the response of polymers such as nylon to tensile impact under conditions in which both the strain and the rate of strain are large, and conventional methods of analysis are inadequate.

The present report describes the situation when the work was begun, explains the mathematical method that was developed, and shows the results of applying the new method to strain propagation in a linear material (one having a stress-strain curve of constant slope) with no creep or other time dependence. The new method is an iterative procedure in which the values are calculated at a network or lattice of points in the position-time plane. The initial conditions and the impact velocity give the values of desired quantities at certain of these lattice points; the propagation of the stress and strain into the lattice is given by the iterative procedure.

Since the solution of the linear problem is known, the present report is essentially a demonstration of the validity of the new method. In subsequent reports the method is applied to problems of greater complexity, including some for which satisfactory solutions have not been previously available.

2. Introduction

A satisfactory theory of the response of materials to loading should permit us to calculate the stresses and strains in a material, for any rate of loading, from a few fixed properties or parameters of the material. There is some latitude in the choice of these fixed properties or parameters and those appropriate for small strains are not necessarily the most convenient when large strains are to be dealt with.

Linear viscoelastic theory is based on the concepts of Hookean "springs" and Newtonian "dashpots". It leads to a complex modulus of elasticity in which the real part is called the storage modulus and the imaginary part the loss modulus. It accounts for both elastic and inelastic deformations including creep, relaxation, and recovery. It holds for slow and rapid deformations, including continuous oscillations. It fails for large strains, however, whether these are produced slowly or rapidly, because the properties of a material at large strains are no longer linear.

Large strains produced at slow or moderate rates may be described by stress-strain curves. A family of curves, each one appropriate to a different rate of straining, will normally be required. Creep or relaxation curves may also be useful; the principle of time-temperature equivalence is sometimes useful when curves taken at slow rates of strain are to be used at higher rates of strain.

When strains are produced rapidly, inertial effects become important. The strains can no longer be considered as uniformly distributed throughout a sample; they propagate as pulses (wave-fronts) that are subject to reflection and attenuation. When inertial effects begin to dominate, it is natural to try a treatment that emphasizes these effects. One way to do this is by formally assuming that stress is a function of strain but is independent of time. With this simplification the propagation of stress and strain within a material may be calculated by the method of characteristics, as has been shown by Von Karman [1], Taylor [2], and Rachmatulin [3]. This method of attack was first applied to metals and has achieved some success. Since time-dependent effects are much more obvious in polymers than in metals, we should perhaps expect the rate-independent theory to be less satisfactory for polymers. However, when the strain-rate is high

it is quite conceivable that the stress would be almost entirely determined by the strain and would depend only slightly on the time elapsed after the strain had been created.

The rate-independent theory as developed by Von Karman has been applied to polymers in these Laboratories and elsewhere, but it is not very satisfactory. Pilsworth and Hoge [4], and Pilsworth [5] have reported measurements in which rubber and nylon were subjected to tensile impact. In a typical experiment on nylon a sample 50 cm long was impacted at 90 m sec^{-1} . Taking 2400 m sec^{-1} as the average velocity of propagation of strain in nylon, the strain pulse produced by the impact had a magnitude of about $90/2400 \approx 3.75$ percent. This is $1/4$ of the breaking strain, which is about 15 percent for nylon. The strain pulse traversed the yarn several times; during the third reflection the yarn broke. Method-of-characteristics calculations were made for the experiment, using several different stress-strain curves. The results showed that any one of several stress-strain curves would predict the observed strain pattern roughly but there was no reasonable stress-strain curve that would explain the observations accurately.

In a typical experiment on rubber, Pilsworth and Hoge impacted a 50 cm length at 42 m sec^{-1} . Taking 50 m sec^{-1} as the average velocity of propagation of strain in rubber, the strain pulse produced by the impact had a magnitude of about $50/42 = 119$ percent. This is a little less than $1/4$ the breaking strain, which for the type of rubber used is about 500 percent. The strain pulse traversed the sample several times; breakage occurred during the third reflection as it had for nylon. Method-of-characteristics calculations were made, again using several different stress-strain curves. Again the conclusion was reached that there was no reasonable stress-strain curve that would give an accurate representation of the observed strain pattern on the basis of time-independent theory. The strain patterns obtained for rubber as described above were modified by making a correction for creep. This improved the agreement between observation and calculation but the modification was tedious and not very elegant.

In both of the experiments cited above, the strain pulse was roughly $1/4$ of the breaking strain, although the pulse in the rubber was 32 times as large as the pulse in the nylon. Both of these pulses we characterize as large, because each is an appreciable fraction of

the breaking strain. The "best" stress-strain curve for use in each of the experiments described above was a derived curve, not a directly measured one. It was selected simply because it gave better results than other curves in the calculation of strain patterns. The curves found in this way are steeper and have a greater curvature than stress-strain curves measured conventionally at low rates of strain. The evidence is fairly strong that time-dependence should not be ignored, and that when it is ignored the stress-strain curve is distorted to partially compensate for it.

The work of Smith and co-workers also establishes the importance of time-dependence at high rates of strain. For example, Smith and Fenstermaker [6] studied the longitudinal strain in rubber subjected to transverse impact. They found significant creep at the point of impact during the first millisecond. During the next 7 milliseconds creep effects were small, but the creep occurring after 8 milliseconds could not be ignored.

Evidence such as that given above brought us to the conclusion that a time-independent theory was inadequate for polymers and that some method should be found to include time-dependence from the start. Such a method is presented in a series of three reports, of which this is the first.

From a mathematical standpoint, the basic idea consists of transforming the relevant partial differential equations into integral equations, and then solving these by a modified method of successive substitutions. The resulting method does not require linearity, and is applicable to systems containing nonlinear and time-dependent materials. In the present report, however, it is applied only to the case where a stress-strain curve exists and is linear, the purpose being to develop the integral equation method, and check the accuracy of the results which it gives by comparing them with the corresponding exact results obtained by other methods. This report also contains some preliminary work which is relevant to time dependent systems.

Since a clear picture of the overall problem must await the appearance of the second and third reports of this series, it should be kept in mind that our primary objective is not to devise a new method for solving linear problems or for solving those nonlinear

problems which can be solved by other methods, but to devise a method capable of solving nonlinear problems involving time-dependent materials. Aside from this, however, the integral equation method developed is new, should be a useful tool in solving other problems, and hence should itself be of interest.

The integral equation approach was chosen because integral equation methods have given good results in the past when used to solve problems involving one or more ordinary differential equations. In those problems integral equations were used in preference to difference equations because of the greater accuracy of numerical integration as compared with numerical differentiation. It is also recognized that methods based on characteristics have been applied to somewhat similar problems [7], and could conceivably lead to useful solutions of the present problem.

3. Statement of Problem. Preliminary Considerations.

The present investigation pertains to the material properties of nylon, rubber, and, perhaps, other substances. The first problem which we shall consider is that of determining the motion of a string of length L and cross-section area A . In the experimental work, a typical value of L was 50 cm. In the case of rubber, the cross section was square, about $1/8$ inch \times $1/8$ inch; in the case of nylon, it was circular, with a diameter of about .05 cm (1050 denier). This string is fixed at the left end, and is initially at rest. At time $t = 0$ the right end is given a velocity v_0 toward the right, as indicated in Fig. 1. For the present v_0 will be held constant. In order to

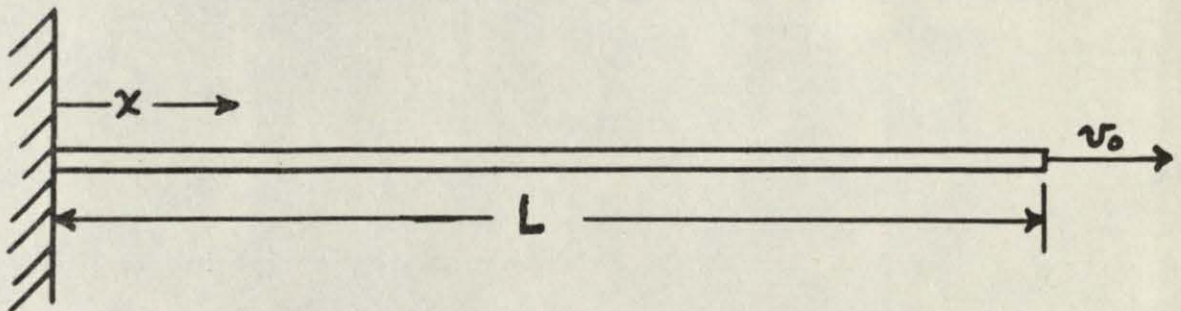


Fig. 1 String subjected to tensile impact.

calculate the subsequent motion of the string, it is necessary that the elastic properties of the material be specified completely. If they are not known they can be assumed, and the validity of the assumptions checked by comparing the resulting calculated motion with that determined experimentally.

Recalling the distinction between plane stress and plane strain in elasticity theory, we note that the present problem involves one-dimensional stress, but not one-dimensional strain. A slab of material constrained to have a fixed cross-section would, on the contrary, if given a constant normal stress over its surfaces have a state of one-dimensional strain, but not one-dimensional stress.

Denoting the normal stress along the axis of the string by σ , and the normal strain along this axis by ϵ , we have as a first approximation the relation

$$\sigma = E\epsilon, \quad (1)$$

given by Hooke's law, E being the constant "modulus of elasticity". The strains perpendicular to the axis of the string may be large, but it will not be necessary to treat them explicitly. They play a role in determining the value of E . Although (1) is adequate for many purposes we wish to consider and to devise mathematical methods for using more accurate stress-strain relationships. Let us consider a few possible improvements in (1).

First, any viscous opposition to the establishment of the strain system would give rise to a stress contribution which is proportional to the time rate of change of strain, thus

$$\sigma = a\epsilon + b \frac{d\epsilon}{dt} \quad (2)$$

where a and b are constants. This relation would correspond to a spring paralleled by a viscous damper, the latter being indicated by a dashpot, Fig. 2.

Second, the coefficient E in (1) may not be constant, but may depend upon ϵ , thus

$$\sigma = E(\epsilon) \epsilon. \quad (3)$$

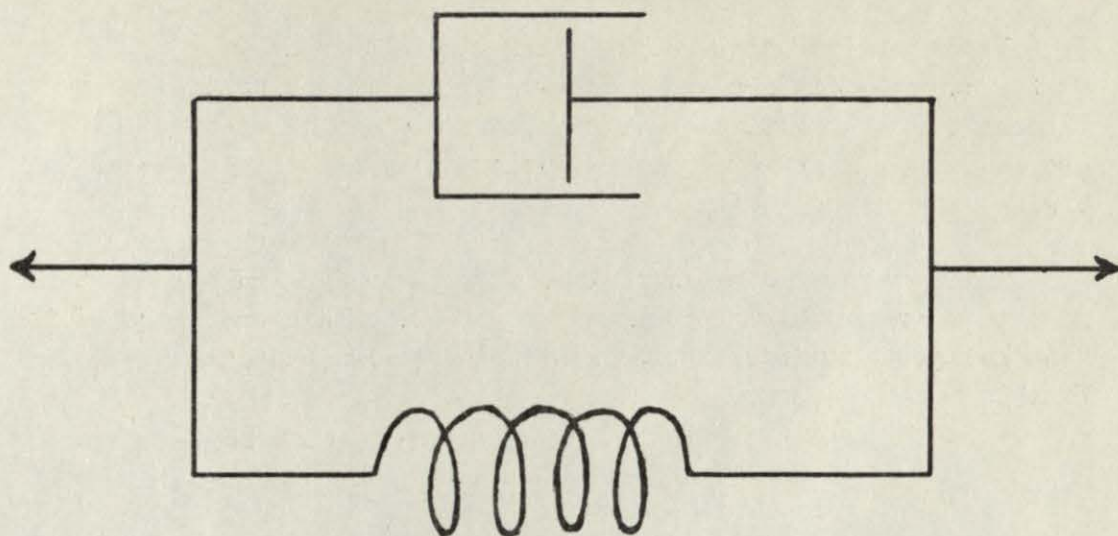


Fig. 2 Viscoelastic model consisting of a spring paralleled by a dashpot.

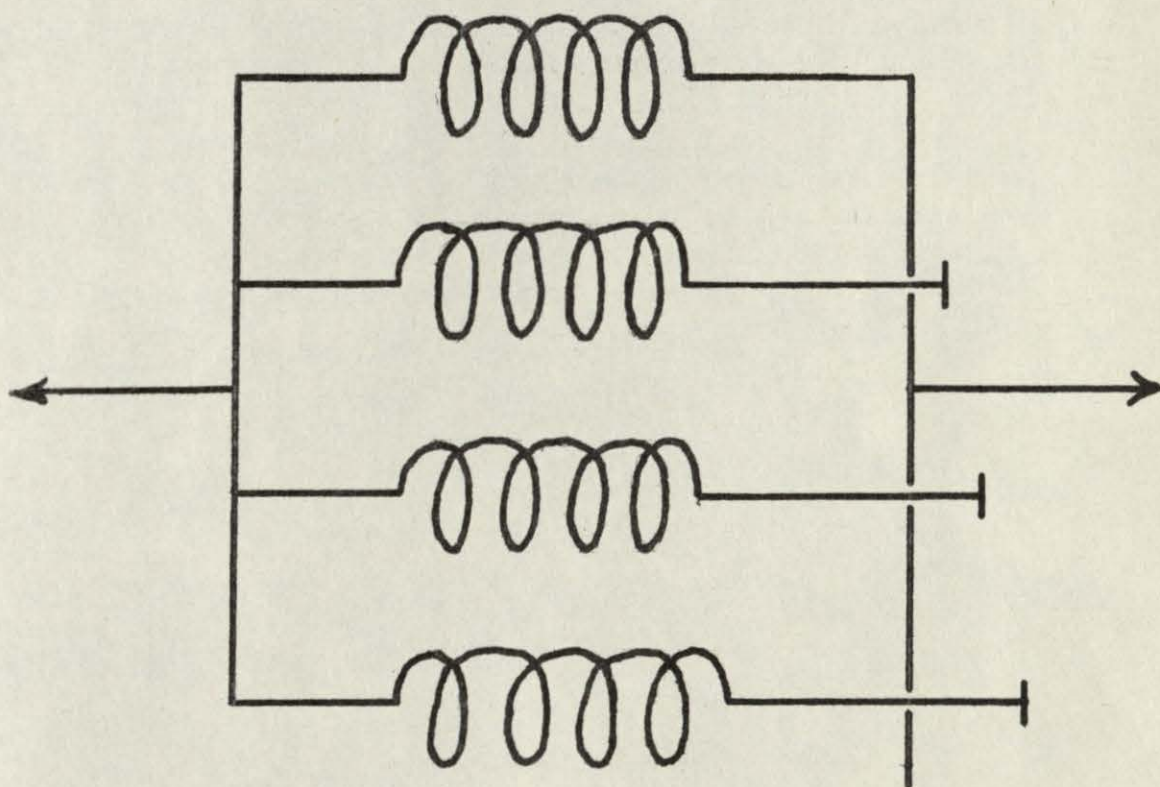


Fig. 3 Model in which the modulus E increases with strain.

It follows that the stress-strain relationship is no longer linear. If the stress-strain curve is concave upward it may be convenient to consider this relation to correspond to a set of springs which are in parallel, and are engaged successively as ϵ is increased, Fig. 3.

Third, we may have a situation wherein an applied stress gives rise to a strain which is composed of two contributions: one of the kind indicated by (1), and the other of the kind indicated by (2). We thus have

$$\begin{aligned}\epsilon &= \epsilon_1 + \epsilon_2, \\ \sigma &= a\epsilon_1, \\ \sigma &= b\epsilon_2 + c \frac{d\epsilon_2}{dt}, \quad \epsilon_2 = 0 \text{ when } t = 0;\end{aligned}\tag{4}$$

which corresponds to two springs in series, one being paralleled by a viscous damper, Fig. 4. In this case a suddenly applied stress gives rise to an immediate proportional strain plus a subsequent creep.

Fourth, it is more than likely that the representation of the stress-strain relationship can be improved by using more complicated systems, whose equivalent mechanical network consists of some series-parallel or even more complicated arrangement of springs and viscous dampers, Fig. 5, for example.

Corresponding to Fig. 5 we have

$$\left. \begin{aligned}\sigma &= \sigma_1 + \sigma_2, \\ \epsilon &= \epsilon_1 + \epsilon_2 = \epsilon_3 + \epsilon_4, \\ \sigma_1 &= a\epsilon_1, \\ \sigma_1 &= b\epsilon_2 + c \frac{d\epsilon_2}{dt}, \quad \epsilon_2 = 0 \text{ when } t = 0, \\ \sigma_2 &= e\epsilon_3, \\ \sigma_2 &= f \frac{d\epsilon_4}{dt}, \quad \epsilon_4 = 0 \text{ when } t = 0,\end{aligned}\right\}\tag{5}$$

where a, b, \dots, f are constants. Finally we note that the mechanical circuit elements need not be lumped - they may be

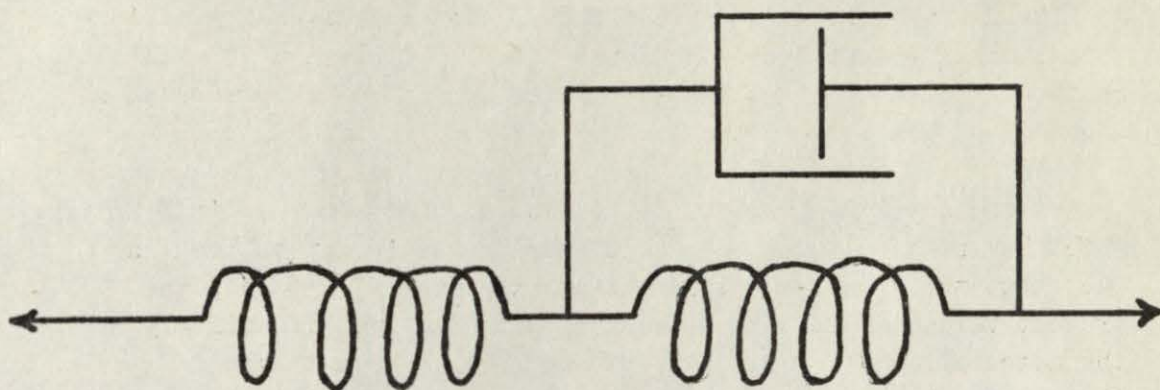


Fig. 4 Three-element viscoelastic model.

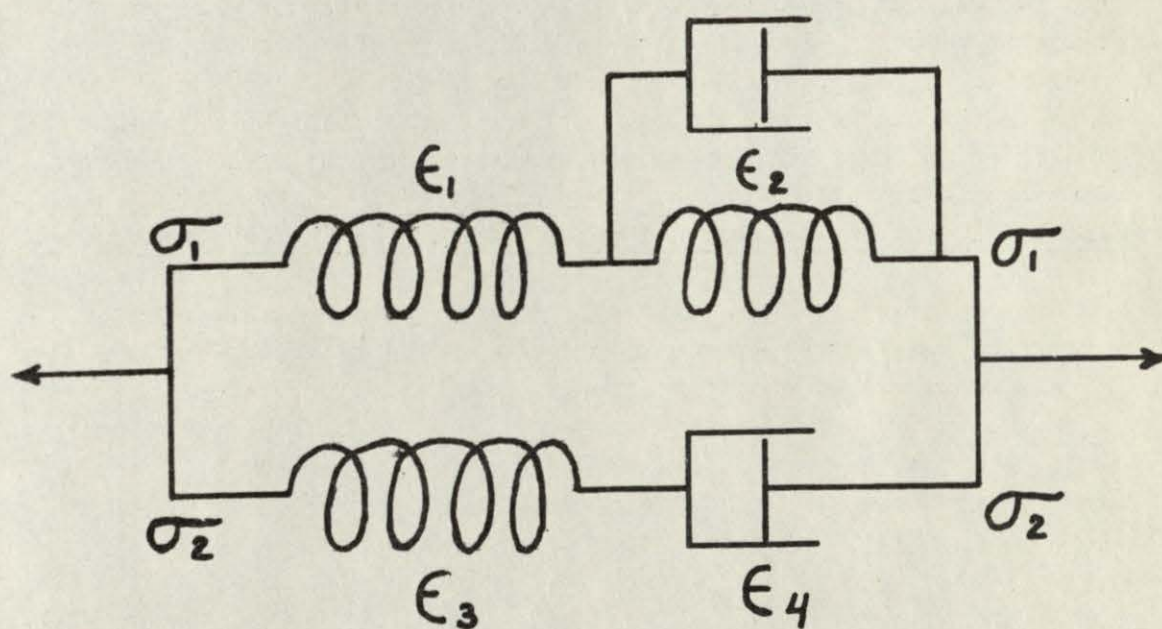


Fig. 5 Multi-element viscoelastic model.

distributed, as in the mechanical analog of an electric cable.

The difficulties which arise in applying a nonlinear relationship such as (3) will be considered later. At present it will be mentioned only that a nonlinear problem can often be treated as a sequence of linear problems.

We are now in a position to foresee another kind of difficulty, which has nothing to do with nonlinearity. This arises from the fact that the stress-strain relationship involves not only the present values of stress and strain, but also the past history of the material. More explicitly we see that whereas in the case of (1) or (3) the present value of the strain determines the stress, and vice versa, this is not true in the other cases which we have just considered. For example, in the case of (2) if a constant stress σ be applied, the strain changes from its initial value zero to its final value, but not abruptly. The difference between the two values dies out exponentially. Conversely the present value of ϵ is not sufficient to determine σ ; $d\epsilon/dt$ is also required. Similar remarks apply in the case of (4), (5), and more complicated cases. This situation is sufficient to explain, and to allow the inclusion of the phenomena of hysteresis and creep. Stated briefly, an elementary piece of material behaves not like a single element in a mechanical network, but like a mechanical system.

In our problem, σ and ϵ are functions of time. It is of interest to take the Laplace transforms of the equations for the models we have been considering, since all show an interesting Hooke's law formalism after transformation. We shall suppose that σ and ϵ are both identically zero before the disturbance. Denoting the Laplace transform of any quantity by a bar over that quantity we obtain from (1) by taking the Laplace transform

$$\bar{\sigma} = E\bar{\epsilon} . \quad (6)$$

Similarly (2) gives

$$\bar{\sigma} = a\bar{\epsilon} + b p \bar{\epsilon} ,$$

or

$$\bar{\sigma} = (a + bp)\bar{\epsilon} . \quad (7)$$

In the case of (4) we obtain

$$\begin{aligned}\bar{\epsilon} &= \bar{\epsilon}_1 + \bar{\epsilon}_2 , \\ \bar{\sigma} &= a\bar{\epsilon}_1 , \\ \bar{\sigma} &= b\bar{\epsilon}_2 + cp\bar{\epsilon}_2 ;\end{aligned}$$

whence

$$\bar{\epsilon} = \frac{\bar{\sigma}}{a} + \frac{\bar{\sigma}}{b + cp} ,$$

or

$$\bar{\sigma} = \frac{a(b + cp)}{a + b + cp} \bar{\epsilon} . \quad (8)$$

Finally, (5) becomes

$$\begin{aligned}\bar{\sigma} &= \bar{\sigma}_1 + \bar{\sigma}_2 , \\ \bar{\epsilon} &= \bar{\epsilon}_1 + \bar{\epsilon}_2 = \bar{\epsilon}_3 + \bar{\epsilon}_4 , \\ \bar{\sigma}_1 &= a\bar{\epsilon}_1 , \\ \bar{\sigma}_1 &= (b + cp) \bar{\epsilon}_2 , \\ \bar{\sigma}_2 &= e\bar{\epsilon}_3 , \\ \bar{\sigma}_2 &= fp\bar{\epsilon}_4 .\end{aligned}$$

It follows that

$$\begin{aligned}\bar{\epsilon} &= \frac{\bar{\sigma}_1}{a} + \frac{\bar{\sigma}_1}{b + cp} = \frac{\bar{\sigma}_2}{e} + \frac{\bar{\sigma}_2}{fp} , \\ \bar{\sigma}_1 &= \frac{a(b + cp)}{a + b + cp} \bar{\epsilon} \\ \bar{\sigma}_2 &= \frac{efp}{e + fp} \bar{\epsilon} ,\end{aligned}$$

whence

$$\bar{\sigma} = \frac{a(b + cp)}{a + b + cp} + \frac{efp}{e + fp} \bar{\epsilon} . \quad (9)$$

It can now be seen that (6), (7), (8), and (9) are all of the form of Hooke's law; but now the proportionality factor between

$\bar{\sigma}$ and $\bar{\epsilon}$ is a function of p . More generally for any linear system let $\bar{E}(p)$ denote the Laplace transform of the stress which results from a unit instantaneous strain impulse applied at $t = 0$, then for any applied stress-time function

$$\bar{\sigma} = \bar{E}(p)\bar{\epsilon} ; \quad (10)$$

(6), (7), (8), and (9) are special cases of this more general relationship. The Laplace transform approach to the problem will not be developed further.

If instead of working with Laplace transforms we work directly with σ and ϵ , we should have to deal with the stress-strain relationship

$$\sigma(t) = \int_0^t E(t-\tau) \epsilon(\tau) d\tau \quad (11)$$

where $E(t)$ is the stress due to a unit strain impulse, and is the inverse transform of $\bar{E}(p)$. Equation (11) is evidently more complicated than (10), and consists of a superposition integral.

4. Partial Differential Equation Approach.

Our general procedure will be to examine the available mathematical methods, and, starting with simpler problems, try to solve problems of increasing difficulty. To have a definite starting point, let us choose the simplest stress-strain relationship (1), namely

$$\sigma = E\epsilon$$

where E is constant, and apply it to the system shown in Fig. 1. In this system let

$$\left. \begin{aligned} L &= \text{length of material unstretched,} \\ A &= \text{cross section of material unstretched,} \\ \rho &= \text{density of material unstretched,} \\ v_0 &= \text{constant velocity of right end of material,} \\ x &= \text{distance from left end, unstretched,} \\ s &= \text{displacement of the particle of material which was} \\ &\quad \text{initially (in the unstretched state) at distance } x \\ &\quad \text{from the left end, } s \text{ is measured positive to the} \\ &\quad \text{right.} \end{aligned} \right\} \quad (12)$$

In setting up the partial differential equation we consider the translatory equilibrium of an infinitesimal interval dx of the unstretched piece of material, Fig. 6. Noting (1) and the fact

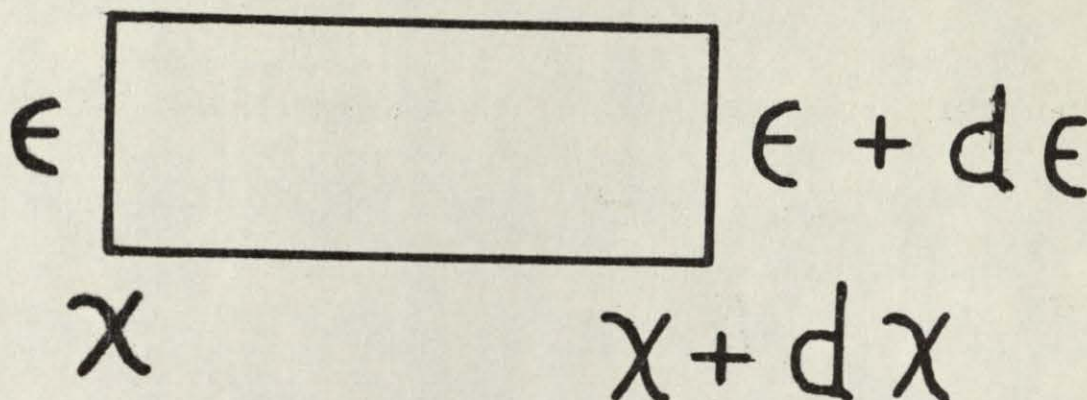


Fig. 6 Infinitesimal element of impacted string.

that

$$\epsilon = \frac{\partial s}{\partial x}, \quad (13)$$

s being a function of x and the time t , we see that the force acting to the left on the left face of the element is $AE \frac{\partial s}{\partial x}$. That acting to the right on the right face of the element is given by a similar expression, the only difference being that $\frac{\partial s}{\partial x}$ must be evaluated at $(x + dx)$ instead of at x . Since

$$\left(\frac{\partial s}{\partial x}\right)_{x+dx} = \frac{\partial s}{\partial x} + \frac{\partial^2 s}{\partial x^2} dx \quad (14)$$

good through first order terms in dx , it follows that the net translatory force on the element that arises because of the stretching is

$$AE \left(\frac{\partial s}{\partial x} + \frac{\partial^2 s}{\partial x^2} dx \right) - AE \frac{\partial s}{\partial x} = AE \frac{\partial^2 s}{\partial x^2} dx. \quad (15)$$

For dynamic equilibrium this force must equal the mass of the element times its acceleration, or

$$\rho A \, dx \, \frac{\partial^2 s}{\partial t^2} . \quad (16)$$

Equating (15) and (16) and canceling $A dx$, we obtain finally

$$\frac{\partial^2 s}{\partial x^2} = \frac{1}{c^2} \frac{\partial^2 s}{\partial t^2} \quad (17)$$

where

$$c = \sqrt{\frac{E}{\rho}} ; \quad (18)$$

(17) is the one-dimensional wave equation, the wave velocity being c . The general solution is

$$s = f(x - ct) + g(x + ct) , \quad (19)$$

which consists of two waves of arbitrary shape traveling with velocity c , one toward the right and one toward the left [8].

In order to apply (19) to the present problem we shall consider x to extend from $-\infty$ to ∞ , and shall determine f and g so that

$$\left. \begin{aligned} s = 0, \quad \frac{\partial s}{\partial t} = 0 \text{ if } 0 \leq x < L, \quad t = 0 ; \\ s = 0 \text{ if } x = 0, \text{ and } \frac{\partial s}{\partial t} = v_0 \text{ if } x = L \text{ for any } t. \end{aligned} \right\} \quad (20)$$

Equation (19) then gives the desired solution for $0 \leq x \leq L$. The first two relations in (20) give

$$\left. \begin{aligned} 0 &= f(x) + g(x) , \\ 0 &= -cf'(x) + cg'(x) , \end{aligned} \right\} 0 \leq x < L, \quad (21)$$

where the primes indicate differentiation. Canceling c and integrating the second of these relations, (21) becomes

$$\left. \begin{aligned} 0 &= f(x) + g(x) , \\ 0 &= -f(x) + g(x) + c_1, \end{aligned} \right\} 0 \leq x < L, \quad (22)$$

where c_1 is an integration constant. Adding and subtracting these equations now gives

$$\left. \begin{aligned} f(x) &= \frac{c_1}{2} , \\ g(x) &= -\frac{c_1}{2} , \end{aligned} \right\} 0 \leq x < L ; \quad (23)$$

c_1 evidently contributes nothing to (19), and will hence be placed equal to zero, giving

$$f(x) = 0, \quad g(x) = 0 \quad \text{if } 0 \leq x < L . \quad (24)$$

Since $f(x-ct)$ gives a wave traveling to the right, and $g(x+ct)$ gives one traveling to the left, we see that in addition to the interval $0 \leq x < L$, $f(x)$ must be determined for all negative values of x , and $g(x)$ must be determined for all positive values of x . These two tasks are essentially the same, however, for the third condition in (20) gives

$$0 = f(-ct) + g(ct); \quad (25)$$

hence

$$f(-x) = -g(x) \quad (26)$$

The last condition in (20) may be written

$$s = v_0 t \text{ when } x = L . \quad (27)$$

Equation (19) in this gives

$$v_0 t = f(L-ct) + g(L+ct) . \quad (28)$$

Using (26) and (28) we can now determine $f(x)$ and $g(x)$ as follows.

Let us construct $f(x)$ and $g(x)$, working outward on both sides from the interval $0 \leq x < L$; and let both $f(x)$ and $g(x)$ be drawn using the same axes, Fig. 7. We now proceed as follows.

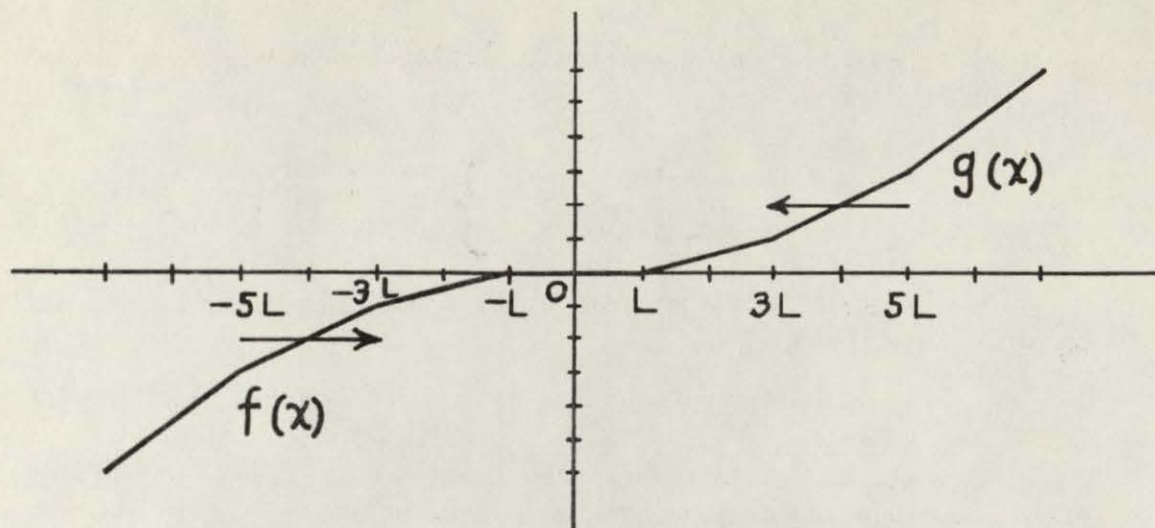


Fig. 7 Functions involved in the general solution of the partial differential equation.

1. Since $g(x) = 0$ if $0 \leq x \leq L$, $f(x) = 0$ for $-L \leq x \leq 0$, due to (26).

2. Noting from (19) that s is given in the interval $0 \leq x \leq L$ by letting the curve $f(x)$ move to the right with velocity c , and the curve $g(x)$ move to the left with velocity c , both starting at $t = 0$; we see that f does not affect s at $x = L$ until it has moved a distance $2L$ to the right. During this time g moves a distance $2L$ to the left, and in order to maintain (27) must slope upward with a slope of v_0/c while passing the point $x = L$; g must therefore slope upward with this slope in the interval $L < x < 3L$, as shown in Fig. 7.

3. It follows now from (26) that f slopes upward with slope v_0/c in the interval $-3L < x < -L$.

4. After f and g have traveled a distance $2L$, f arrives at $x = L$ and would cancel any further growth of s at this point if the slope of g were not altered. In order to maintain the rate of growth of s we increase the slope of g by an amount v_0/c to cancel the effect of f . This maintains the growth of s at $x = L$ while the curves move an additional distance $2L$; $g(x)$ therefore slopes upward with a slope $2v_0/c$ in the interval $3L < x < 5L$.

5. It now follows from (26) that f slopes upward with a slope $2v_0/c$ in the interval $-5L < x < -3L$.

6. After the curves have moved an additional distance $2L$ the portion of f with slope $2v_0/c$ arrives at $x = L$, and it becomes necessary to increase the slope of g by an additional amount v_0/c to give a slope of $3v_0/c$, and so on.

We now see that $g(x)$ consists of a broken line. Beyond the first interval $0 \leq x \leq L$, in which $g(x) = 0$, $g(x)$ consists of a series of straight line segments of horizontal length $2L$ and slopes v_0/c , $2v_0/c$, $3v_0/c$, $4v_0/c$, ... respectively. We also see that $f(x)$ may be obtained by rotating the curve of $g(x)$ 180° about the origin, and hence consists also of a broken line, Fig. 7.

To obtain $s(x,t)$ we add the ordinate of g at abscissa $(x+ct)$ to that of f at abscissa $(x-ct)$, as indicated by (19). We see, however, that if $ct > x$, the ordinate of f at abscissa $x-ct$ is the negative of the ordinate of g at abscissa $(ct-x)$. Since if $ct < x$ the contribution of f to s is zero, it now follows that $f(x)$ can be discarded, and $s(x,t)$ determined from $g(x)$ as indicated in Fig. 8.

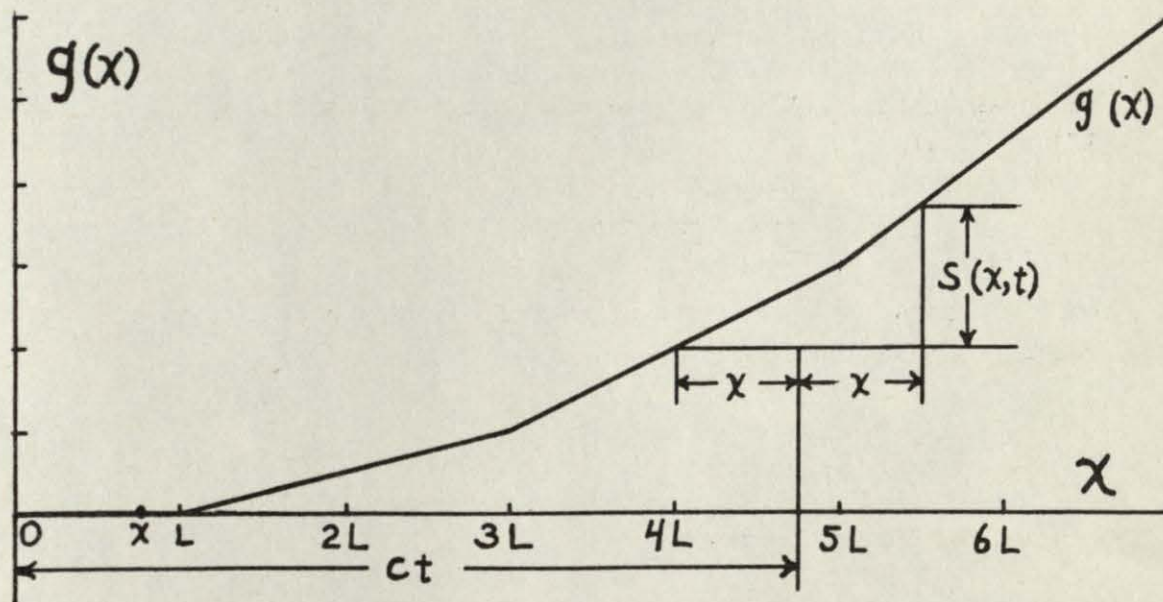


Fig. 8 Illustration showing how $s(x,t)$ may be obtained from $g(x)$.

If we reduce ct we see that when it reaches x we have already lost any contribution by f . The above construction for s can hence be rendered valid for values of ct right down to zero by extending $g(x)$ into the interval $-L \leq x \leq 0$ and placing

$$g(x) = 0 \quad \text{if } -L \leq x \leq 0. \quad (29)$$

It may finally be mentioned that a similar procedure could be devised if v_0 were not constant, but a given function of t .

Fourier Series Solution.

The problem we have just solved can also be solved by using Fourier technique. The result obtained will be less general, but it will be needed to validate some of the practical formulas to be obtained later. In order to apply Fourier technique it is necessary to get rid of the nonhomogeneous boundary condition at the right hand end of the string, namely the condition

$$\frac{\partial s}{\partial t} = v_0 \quad \text{when } x = L. \quad (30)$$

In order to do this we place

$$s = \frac{v_0 x t}{L} + s_1 \quad (31)$$

and consider the problem of determining s_1 . Substituting (31) in (17) we obtain

$$\frac{\partial^2 s_1}{\partial x^2} = \frac{1}{c^2} \frac{\partial^2 s_1}{\partial t^2} ; \quad (32)$$

hence s_1 satisfies the same partial differential equation as s . Writing (31) in the form

$$s_1 = s - \frac{v_0 x t}{L}, \quad (33)$$

and substituting from (20), we obtain the following initial and boundary conditions on s_1 :

$$\left. \begin{aligned}
 s_1 &= 0 \text{ when } t = 0, 0 \leq x \leq L, \\
 \frac{\partial s_1}{\partial t} &= -\frac{v_0 x}{L} \text{ when } t = 0, \\
 s_1 &= 0 \text{ when } x = 0, \quad t \geq 0, \\
 s_1 &= 0 \text{ when } x = L, \quad t \geq 0.
 \end{aligned} \right\} (34)$$

Proceeding in the usual manner we obtain particular solutions of (32) of the form

$$s_{1p} = X(x) T(t); \quad (35)$$

(35) in (32) gives

$$X'' T = \frac{1}{c^2} X T'' ,$$

or

$$\frac{X''}{X} = \frac{1}{c^2} \frac{T''}{T} = -k^2 = \text{constant} \quad (36)$$

since $\frac{X''}{X}$ is a function of x alone, and $\frac{T''}{T}$ is a function of t alone.

Then (36) gives

$$\left. \begin{aligned}
 X'' + k^2 X &= 0, \\
 T'' + k^2 c^2 T &= 0.
 \end{aligned} \right\} (37)$$

Since both of these equations are linear and have constant coefficients we can write down the solutions immediately, thus

$$\left. \begin{aligned}
 X &= c_1 \sin kx + c_2 \cos kx, \\
 T &= c_3 \sin ket + c_4 \cos ket.
 \end{aligned} \right\} (38)$$

Placing

$$\left. \begin{aligned}
 c_2 &= 0, \\
 k &= \frac{n\pi}{L}, \quad n = 1, 2, 3, \dots,
 \end{aligned} \right\} (39)$$

we satisfy the end conditions in (34); and placing

$$c_4 = 0 \quad (40)$$

we satisfy the initial condition on displacement. Superimposing the particular solutions given by the various values of n we obtain

$$s_1 = \sum_{n=1}^{\infty} c_n \sin \frac{n\pi x}{L} \sin \frac{n\pi ct}{L}, \quad (41)$$

which expression satisfies the partial differential equation, the end conditions, and the initial condition on displacement. To satisfy the initial condition on velocity we place

$$-\frac{v_0 x}{L} = \left(\frac{\partial s_1}{\partial t} \right)_{t=0} \quad (42)$$

or

$$\begin{aligned} -\frac{v_0 x}{L} &= \sum_{n=1}^{\infty} c_n \frac{n\pi c}{L} \sin \frac{n\pi x}{L}, \\ -\frac{v_0 x}{\pi c} &= \sum_{n=1}^{\infty} c_n n \sin \frac{n\pi x}{L}. \end{aligned} \quad (43)$$

Hence $c_n n$ is the coefficient of $\sin \frac{n\pi x}{L}$ in the Fourier sine series expansion of $(-v_0 x / \pi c)$. It follows that

$$c_n n = \frac{2}{L} \int_0^L -\frac{v_0 x}{\pi c} \sin \frac{n\pi x}{L} dx, \quad (44)$$

$$\begin{aligned} c_n &= -\frac{2v_0}{Ln\pi c} \left[\left(\frac{L}{n\pi} \right)^2 \sin \frac{n\pi x}{L} - \frac{Lx}{n\pi} \cos \frac{n\pi x}{L} \right]_0^L \\ &= \frac{2v_0 L}{n^2 \pi^2 c} \cos n\pi \end{aligned} \quad (45)$$

or

$$c_n = \frac{(-1)^n 2v_0 L}{n^2 \pi^2 c}. \quad (46)$$

Placing (46) in (41), and then (41) in (31), we obtain finally

$$s = v_0 \left(\frac{xt}{L} + \frac{2L}{\pi^2 c} \sum_{n=1}^{\infty} \frac{(-1)^n}{n^2} \sin \frac{n\pi x}{L} \sin \frac{n\pi ct}{L} \right). \quad (47)$$

This expression gives s as the sum of a steady proportional stretching and a set of vibrations in natural modes at successively higher frequencies.

5. Integral Equation Approach. Conversion of the Differential Equation, and Solution by Successive Substitutions.

Since we do not wish to limit ourselves to the solution of linear problems, and since none of the solutions so far presented furnishes a suitable means of dealing with nonlinear or time-dependent materials, our main problem is not yet solved. The integral equation approach, which will now be presented, has in the past led to the solution of a variety of nonlinear problems. The differential equation is converted to an integral equation, and the integral equation is then solved by successive substitutions. The problems solved in the past by this technique involved but a single independent variable, and the corresponding differential equations were ordinary; whereas in the present problem two independent variables are involved, and the differential equation is partial. Nevertheless, let us try this approach and see what happens. In so doing it is desirable first to devise the method and apply it to a few problems whose solutions are known, before attacking the main problem.

Accordingly, let us first consider the case where the string extends from minus infinity to plus infinity. Noting (17), (18), and (12) we see that the differential equation for longitudinal motion is

$$\frac{\partial^2 s}{\partial t^2} = c^2 \frac{\partial^2 s}{\partial x^2} \quad (48)$$

where for the present we consider c to be constant. As initial conditions let us place

$$s(x, 0) = f(x), \quad \left(\frac{\partial s}{\partial t}\right)_{t=0} = 0, \quad (49)$$

corresponding to which the initial displacement at x is $f(x)$, and the initial velocity is zero. Integrating (48) twice with respect to t we obtain

$$\frac{\partial s}{\partial t} = \left(\frac{\partial s}{\partial t}\right)_{t=0} + c^2 \int_0^t \frac{\partial^2 s}{\partial x^2} dt, \quad (50)$$

$$s = s(x, 0) + t \left(\frac{\partial s}{\partial t}\right)_{t=0} + c^2 \int_0^t \int_0^t \frac{\partial^2 s}{\partial x^2} dt dt. \quad (51)$$

With the initial conditions (49) this becomes

$$s = f(x) + c^2 \int_0^t \int_0^t \frac{\partial^2 s}{\partial x^2} dt dt. \quad (52)$$

Putting s equal to an assumed function s_0 in the integrand we obtain a function s_1 for the left hand side; then inserting s_1 in the integrand we obtain s_2 , and so on. We thus have a method of successive substitutions defined by the following set of equations

$$s_{n+1} = f(x) + c^2 \int_0^t \int_0^t \frac{\partial^2 s_n}{\partial x^2} dt dt, n=0, 1, 2, \dots \quad (53)$$

There is, of course, a question of convergence. We hope that ultimately s_{n+1} will differ inappreciably from s_n .

In order to start the process let us place $s_0 = 0$; then (53) gives

$$\left. \begin{aligned} s_1 &= f(x), \\ s_2 &= f(x) + \frac{c^2 t^2}{2} f''(x), \\ s_3 &= f(x) + \frac{c^2 t^2}{2} f''(x) + \frac{c^4 t^4}{4!} f^{iv}(x), \\ s_4 &= f(x) + \frac{c^2 t^2}{2} f''(x) + \frac{c^4 t^4}{4!} f^{iv}(x) + \frac{c^6 t^6}{6!} f^{vi}(x), \\ &\vdots \\ s_n &= f(x) + \frac{c^2 t^2}{2!} f''(x) + \frac{c^4 t^4}{4!} f^{iv}(x) + \dots + \frac{c^{2n-2} t^{2n-2}}{2n-2!} f^{2n-2}(x). \end{aligned} \right\} (54)$$

Ultimately

$$s = f(x) + \frac{c^2 t^2}{2!} f''(x) + \frac{c^4 t^4}{4!} f^{iv}(x) + \frac{c^6 t^6}{6!} f^{vi}(x) + \dots \quad (55)$$

But one form of Taylor's series is

$$\phi(x+h) = \phi(x) + \phi'(x)h + \phi''(x)\frac{h^2}{2!} + \phi'''(x)\frac{h^3}{3!} + \dots \quad (56)$$

It follows that

$$\left. \begin{aligned} f(x+ct) &= f(x) + ct f'(x) + \frac{c^2 t^2}{2!} f''(x) + \dots, \\ f(x-ct) &= f(x) - ct f'(x) + \frac{c^2 t^2}{2!} f''(x) - \dots; \end{aligned} \right\} \quad (57)$$

hence (55) becomes

$$s = \frac{1}{2} [f(x+ct) + f(x-ct)], \quad (58)$$

which is known to be the exact solution of the problem, subject to the usual conditions of convergence. The rate of convergence of the series is important; if the rate is too low the method may not be good for practical use.

As our next problem let us consider the case where the initial displacements are zero and the initial velocity distribution is given, thus instead of (49) we have

$$s(x, 0) = 0, \quad \left(\frac{\partial s}{\partial t} \right)_{t=0} = g(x). \quad (59)$$

The differential equation (48) is still valid; hence integrating twice with respect to t , as before, we obtain (51), which due to (59) becomes

$$s = t g(x) + c^2 \int_0^t \int_0^t \frac{\partial^2 s}{\partial x^2} dt dt. \quad (60)$$

Proceeding as with (53) we introduce a method of successive substitutions described by the equations

$$s_{n+1} = t g(x) + c^2 \int_0^t \int_0^t \frac{\partial^2 s_n}{\partial x^2} dt dt, \quad n = 0, 1, 2, \dots \quad (61)$$

Starting the process by placing $s_0 = 0$, (61) gives

$$\left. \begin{aligned}
 s_1 &= t g(x), \\
 s_2 &= t g(x) + \frac{c^2 t^3}{3!} g''(x), \\
 s_3 &= t g(x) + \frac{c^2 t^3}{3!} g''(x) + \frac{c^4 t^5}{5!} g^{iv}(x) \\
 &\cdot \quad \cdot \quad \cdot \quad \cdot \quad \cdot \quad \cdot \quad \cdot \quad \cdot \quad \cdot \quad \cdot \\
 s_n &= t g(x) + \frac{c^2 t^3}{3!} g''(x) + \dots + \frac{c^{2n-2} t^{2n-1}}{2n-1!} g^{(2n-2)}(x)
 \end{aligned} \right\} \quad (62)$$

Ultimately

$$s = t g(x) + \frac{c^2 t^3}{3!} g''(x) + \frac{c^4 t^5}{5!} g^{iv}(x) + \dots \quad (63)$$

Noting (56) and (57) we see that

$$\left. \begin{aligned}
 \int_0^t g(x+ct) dt &= t g(x) + \frac{ct^2}{2!} g'(x) + \frac{c^2 t^3}{3!} g''(x) + \dots, \\
 \int_0^t g(x-ct) dt &= t g(x) - \frac{ct^2}{2!} g'(x) + \frac{c^2 t^3}{3!} g''(x) + \dots;
 \end{aligned} \right\} \quad (64)$$

hence (63) becomes

$$s = \frac{1}{2} \int_0^t [g(x+ct) + g(x-ct)] dt. \quad (65)$$

Placing

$$\left. \begin{aligned}
 u &= x + ct, \\
 du &= c dt,
 \end{aligned} \right\} \quad (66)$$

we obtain

$$\int_0^t g(x+ct) dt = \frac{1}{c} \int_x^{x+ct} g(u) du, \quad (67)$$

also, placing

$$\left. \begin{aligned}
 u &= x - ct, \\
 du &= -c dt,
 \end{aligned} \right\} \quad (68)$$

we obtain

$$\int_0^t g(x-ct) dt = -\frac{1}{c} \int_x^{x-ct} g(u) du. \quad (69)$$

Putting equations (67) and (69) in (65) gives finally

$$s = \frac{1}{2c} \int_{x-ct}^{x+ct} g(u) du, \quad (70)$$

which is known to be the exact solution of the problem.

As our last problem of this kind, let us consider the case where the initial distributions of both the displacement and the velocity are given, thus

$$s(x,0) = f(x), \quad \left(\frac{\partial s}{\partial t}\right)_{t=0} = g(x). \quad (71)$$

Equation (51) is now valid, and becomes

$$s = f(x) + t g(x) + c^2 \int_0^t \int_0^t \frac{\partial^2 s}{\partial x^2} dt dt. \quad (72)$$

Our method of successive substitutions is now described by the equations

$$s_{n+1} = f(x) + t g(x) + c^2 \int_0^t \int_0^t \frac{\partial^2 s_n}{\partial x^2} dt dt, \quad n=0, 1, 2, \dots \quad (73)$$

Starting the process by placing $s_0 = 0$ we obtain for s_1, s_2, \dots , respectively, the sums of the corresponding expressions given in (54) and (62). The expression ultimately obtained for s is hence the sum of those given in (55) and (63); and this can evidently be written as the sum of (58) and (70). We thus obtain finally

$$s = \frac{1}{2} [f(x+ct) + f(x-ct)] + \frac{1}{2c} \int_{x-ct}^{x+ct} g(u) du \quad (74)$$

which is known to be the exact solution of the problem for the linear case [8].

Extension to the Case of a Finite Length.

In the above, in order to fix ideas, the piece was considered to be infinite in length; however, since in the successive substitution process both integrations were on t with x held constant, it was not necessary to consider the piece to be infinite, or to extend outside of the interval $0 \leq x \leq L$. Accordingly, let us consider the problem as it is actually given. That is the piece is finite in length, extending from 0 to L ; the end conditions are

$$s(0, t) = 0, \quad \left(\frac{\partial s}{\partial t}\right)_{x=L} = v_0; \quad (75)$$

and the initial conditions are

$$s(x, 0) = 0, \quad 0 \leq x \leq L, \quad (76)$$

$$\left(\frac{\partial s}{\partial t}\right)_{t=0} = 0, \quad 0 \leq x < L, \quad (77)$$

$$\left(\frac{\partial s}{\partial t}\right)_{t=0} = v_0; \quad x = L. \quad (78)$$

We note that $\left(\frac{\partial s}{\partial t}\right)_{t=0}$ is discontinuous when $x = L$.

The integral equation is given by (60) or by (72) with $f(x)$ placed equal to zero in accordance with (76).

We note that $g(x) = \left(\frac{\partial s}{\partial t}\right)_{t=0}$ is given by (77) and (78).

Placing

$$g(x) = \frac{v_0 x}{L} + g_1(x), \quad (79)$$

where

$$\left. \begin{aligned} g_1(x) &= -\frac{v_0 x}{L} \quad \text{if } 0 \leq x < L, \\ g_1(x) &= 0 \quad \text{if } x = L, \end{aligned} \right\} \quad (80)$$

we see that $g_1(x)$ can be expressed completely — including the discontinuity at $x = L$ — by the sine series

$$g_1(x) = \sum_{i=1}^{\infty} a_i \sin \frac{i\pi x}{L} \quad (81)$$

where

$$a_i = \frac{2}{L} \int_0^L g_1(x) \sin \frac{i\pi x}{L} dx. \quad (82)$$

Substituting from (80) this becomes

$$\begin{aligned} a_i &= \frac{2}{L} \int_0^L \left(-\frac{v_0 x}{L}\right) \sin \frac{i\pi x}{L} dx \\ &= -\frac{2v_0}{L^2} \left[\left(\frac{L}{i\pi}\right)^2 \sin \frac{i\pi x}{L} - \frac{Lx}{i\pi} \cos \frac{i\pi x}{L} \right]_0^L \\ a_i &= \frac{2v_0}{i\pi} \cos i\pi = (-1)^i \frac{2v_0}{i\pi}; \end{aligned} \quad (83)$$

hence

$$g_1(x) = \frac{2v_0}{\pi} \sum_{i=1}^{\infty} \frac{(-1)^i}{i} \sin \frac{i\pi x}{L}. \quad (84)$$

This in (79) gives

$$g(x) = \frac{v_0 x}{L} + \frac{2v_0}{\pi} \sum_{i=1}^{\infty} \frac{(-1)^i}{i} \sin \frac{i\pi x}{L}. \quad (85)$$

We now substitute (85) in (60), and then start the successive substitution process by first placing $s=0$. It may be noted that the first term in (85) at no stage contributes anything to the integral. The result of the successive substitution process is

$$\begin{aligned} s &= \frac{v_0 x t}{L} + \frac{2v_0 t}{\pi} \sum_{i=1}^{\infty} \frac{(-1)^i}{i} \sin \frac{i\pi x}{L} \\ &\quad - \frac{2v_0}{\pi} \left(\frac{c\pi}{L}\right)^2 \frac{t^3}{3!} \sum_{i=1}^{\infty} \frac{(-1)^i i^2}{i} \sin \frac{i\pi x}{L} \\ &\quad + \frac{2v_0}{\pi} \left(\frac{c\pi}{L}\right)^4 \frac{t^5}{5!} \sum_{i=1}^{\infty} \frac{(-1)^i i^4}{i} \sin \frac{i\pi x}{L} \\ &\quad - \frac{2v_0}{\pi} \left(\frac{c\pi}{L}\right)^6 \frac{t^7}{7!} \sum_{i=1}^{\infty} \frac{(-1)^i i^6}{i} \sin \frac{i\pi x}{L} + \dots \end{aligned} \quad (86)$$

$$s = \frac{v_0 x t}{L} + \frac{2v_0 L}{c\pi^2} \sum_{i=1}^{\infty} \frac{(-1)^i}{i^2} \sin \frac{ic\pi t}{L} \sin \frac{i\pi x}{L}, \quad (87)$$

which agrees with (47). We thus see that the nonhomogeneous end condition at $x = L$ can be used without alteration, and the piece considered to extend over the finite interval $0 \leq x \leq L$.

In appendixes A and B a method is provided for handling problems in which the motion of the impacted end of the string is arbitrary. This permits us, for example, to specify a finite velocity rise-time, which is more realistic than the zero-rise-time we have been using. The method is based on the superposition principle and requires the material to be linear. The development is given in Appendix A and the corresponding formulas for numerical approximation are given in Appendix B.

Since the method of successive substitutions has been shown to be valid for a linear (Hooke's law) string of finite length, we can feel confident that it will also work when applied to nonlinear, time-dependent materials. The problem will be treated directly in the form in which it is given — that is with a piece of finite length and a nonhomogeneous boundary condition. It is likely that the nonlinearity and creep will not greatly affect the convergence of the process, but will merely complicate the numerical work.

6. Development of Approximate Methods for Solving the Integral Equation by Successive Substitution.

We wish to obtain the solution of the nonlinear problem with creep. To apply the theory developed above, this requires the devising of approximate methods for carrying out the successive substitution process. In so doing the difficulties encountered will very likely be about the same regardless of whether or not we consider nonlinearity and creep; hence in order to keep the amount of numerical work as small as possible, let us first work with the linear problem. Since we have the solution of this problem we can use it as a check on our results, which is an additional advantage.

Nature of the solution of the Linear Problem. Referring to Fig. 8 we see that $s(x,t)$ is given by the increment of g over an interval $2x$ whose midpoint is at abscissa ct . Since $g(x)$ is a broken line it follows immediately that in general $\partial s/\partial x$ and $\partial s/\partial t$ are constant. The same is hence true of the vector

$$i \frac{\partial s}{\partial x} + j \frac{\partial s}{\partial t} - k,$$

whose direction is normal to the surface $s(x, t)$. We thus see that the surface $s(x, t)$ is composed of pieces of planes.

The values of $\partial s / \partial t$ and $\partial s / \partial x$ can, in addition, be determined. In so doing we note that there are two possibilities, (a) and (b).

In (a), $g(x)$ has no corner in the interval of width $2x$. In this case $g(x)$ has a constant slope nv_0/c in the interval. Holding x fixed and increasing t by an amount dt we obtain

$$\begin{aligned} ds &= 0 ; \\ \text{hence } \frac{\partial s}{\partial t} &= 0 . \end{aligned} \quad \left. \vphantom{\begin{aligned} ds &= 0 ; \\ \frac{\partial s}{\partial t} &= 0 . \end{aligned}} \right\} \quad (88)$$

Next, let us hold t fixed and increase x by an amount dx ; then

$$ds = 2n \frac{v_0}{c} dx ;$$

hence

$$\frac{\partial s}{\partial x} = 2n \frac{v_0}{c} . \quad (89)$$

Here n is an integer which is determined by the particular branch of $g(x)$ which we are considering. In case (b), $g(x)$ has a corner in the interval of width $2x$. In this case $g(x)$ consists of two straight lines in the interval, their slopes being $n v_0/c$ and $(n+1) v_0/c$, respectively. Proceeding as before, we hold x constant; then

$$ds = (n+1) \frac{v_0}{c} c dt - n \frac{v_0}{c} c dt$$

$$ds = v_0 dt ;$$

hence

$$\frac{\partial s}{\partial t} = v_0 . \quad (90)$$

Next we hold t constant; then

$$ds = (n+1) \frac{v_0}{c} dx + n \frac{v_0}{c} dx$$

$$ds = (2n+1) \frac{v_0}{c} dx ;$$

hence

$$\frac{\partial s}{\partial x} = (2n+1) \frac{v_0}{c} . \quad (91)$$

It is interesting to note that $\partial s / \partial t$ takes only the values 0 and v_0 , whereas $\partial s / \partial x$ keeps increasing, though by abrupt increments of v_0/c . The outer boundary of the surface $s(x,t)$ consists of three straight lines, namely, the x axis, the t axis, and the line

$$s = v_0 t , \quad x = L. \quad (92)$$

In view of this and the fact that planes intersect in straight lines we see that the various plane portions of the surface $s(x,t)$ are bounded by straight lines.

Referring to Fig. 8 we see that as t increases with x fixed the transition from one plane portion of the surface to the next occurs when either end of the interval of width $2x$ passes a corner of the broken line $g(x)$. Letting x differ but slightly from zero, we see that the transition points on the t axis occur at

$$\begin{aligned} ct &= L, 3L, 5L, \dots, \\ \text{or } t &= \frac{L}{c}, \frac{3L}{c}, \frac{5L}{c}, \dots \end{aligned} \quad (93)$$

Similarly if we let x be slightly smaller than L we see that the transition points on the boundary line (92) are at

$$\begin{aligned} ct &= 0, 2L, 4L, \dots, \\ \text{or } t &= 0, \frac{2L}{c}, \frac{4L}{c}, \dots \end{aligned} \quad (94)$$

Applying the above results, noting (93) and (94), we see that the transition lines between the various plane portions of the surface $s(x,t)$ are as shown in Fig. 9. These lines together with the x axis, the t axis, and the line (92) form the boundaries of these plane portions, and hence determine them. A three-dimensional view of the surface is shown in Fig. 10.

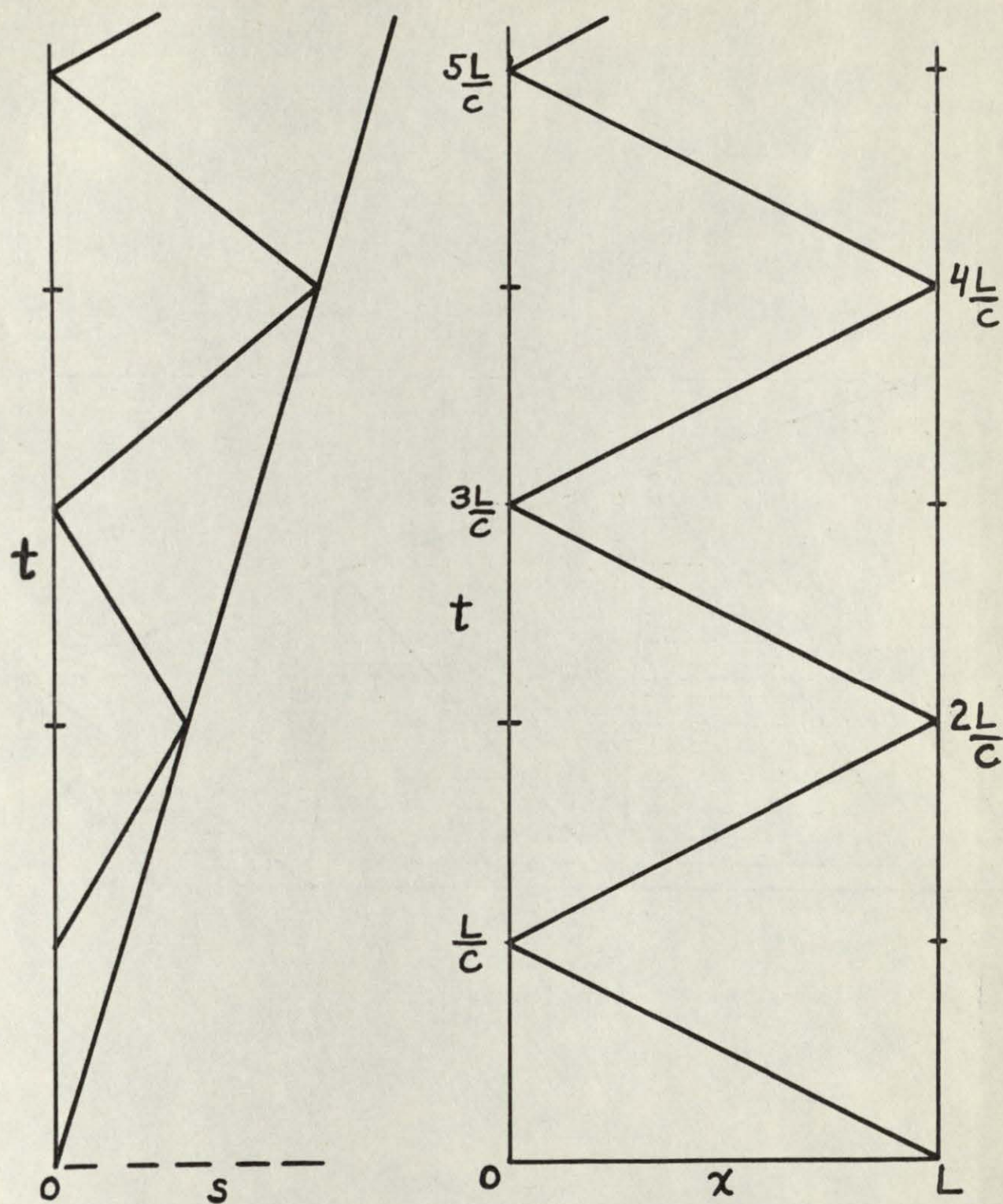


Fig. 9 Views of the surface $s=s(x,t)$, showing transition lines between the plane portions of the surface. At the left is a side view in the $+x$ direction, and at the right is a top view in the $(-s)$ direction.

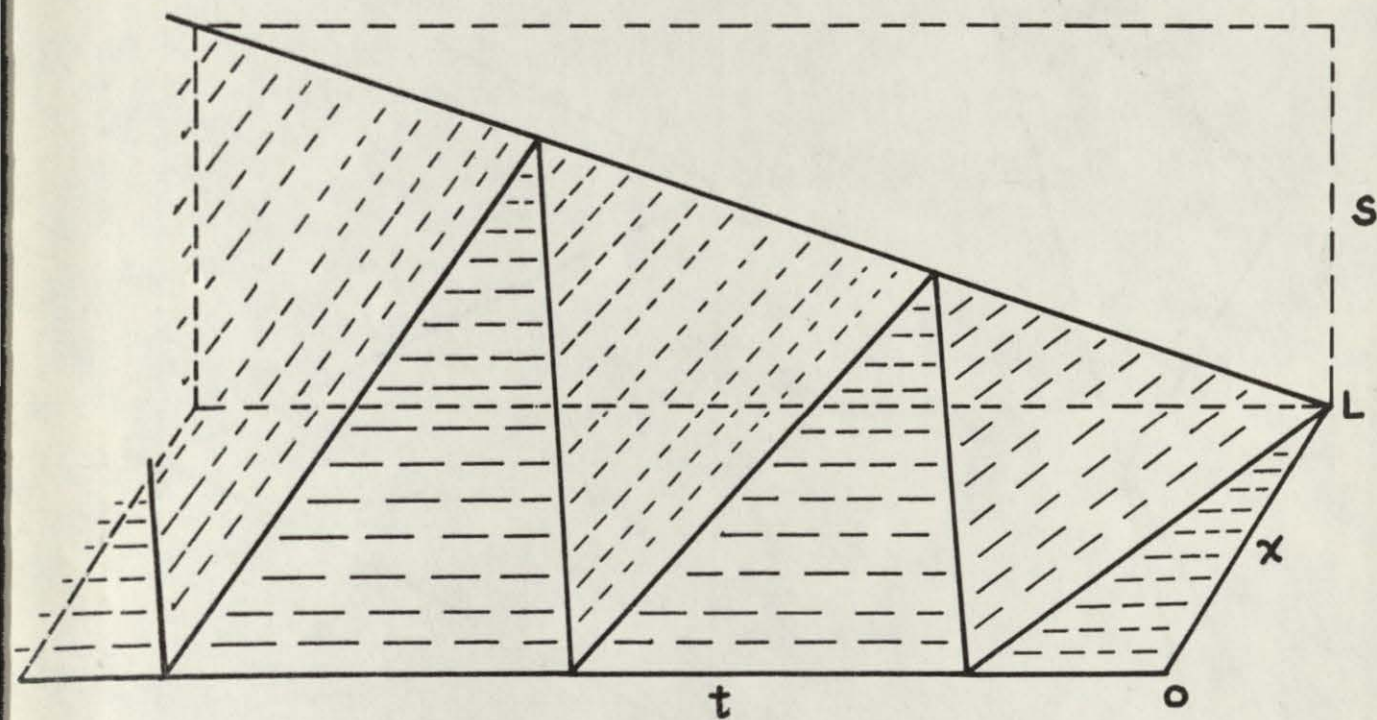


Fig. 10 Three dimensional view of the surface $s(x,t)$

Behavior of the Integral Equation. On each of the plane surfaces which together compose the surface $s(x, t)$ we have

$$\frac{\partial^2 s}{\partial x^2} = 0. \quad (95)$$

It follows that in the integral equation (60), namely

$$s = tg(x) + c^2 \int_0^t \int_0^t \frac{\partial^2 s}{\partial x^2} dt dt,$$

the integrand in the integral vanishes over all of the component plane surfaces. The changes in the first of the two integrals hence take place abruptly at the transition lines between adjacent surfaces.

In order to see what happens at such a line let us consider the cylindrical surface

$$z = f(x). \quad (96)$$

Looking down from above let us consider a ξ axis, which lies in the xy plane and makes an angle α with the x axis, as shown in Fig. 11.

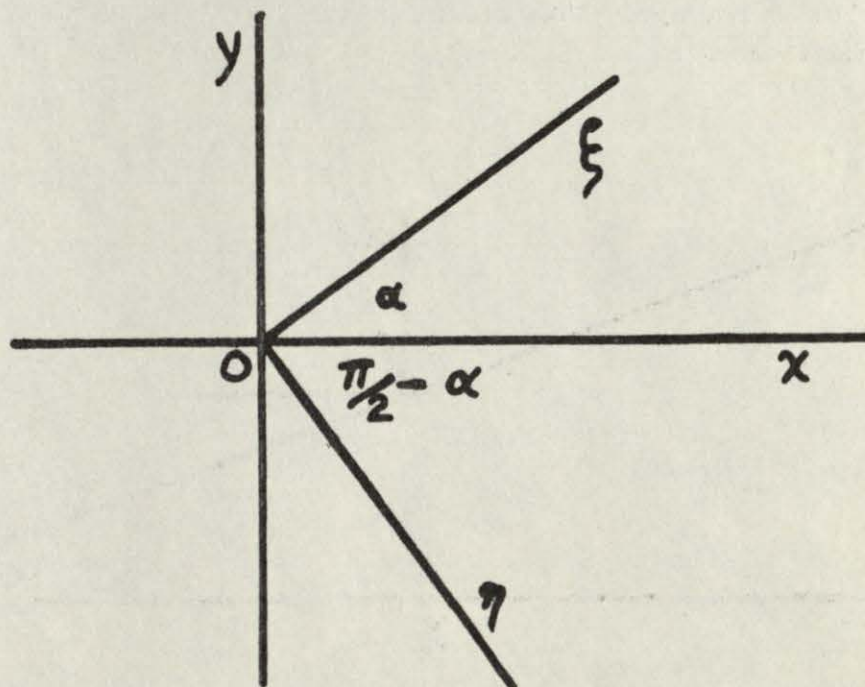


Fig. 11 Diagram for deriving relations satisfied by a cylindrical surface.

Evidently

$$x = \xi \cos \alpha ; \quad (97)$$

hence

$$z = f(\xi \cos \alpha). \quad (98)$$

It follows that

$$\frac{\partial z}{\partial \xi} = f'(\xi \cos \alpha) \cos \alpha, \quad (99)$$

$$\frac{\partial^2 z}{\partial \xi^2} = f''(\xi \cos \alpha) \cos^2 \alpha. \quad (100)$$

Similarly, if we choose an η axis perpendicular to the ξ axis, Fig. 11, we have

$$x = \eta \sin \alpha, \quad (101)$$

$$\frac{\partial^2 z}{\partial \eta^2} = f''(\eta \sin \alpha) \sin^2 \alpha. \quad (102)$$

Noting (97) and (101) we see from (100) and (102) that

$$\frac{\partial^2 z}{\partial \eta^2} = \frac{\partial^2 z}{\partial \xi^2} \tan^2 \alpha. \quad (103)$$

Let us now apply this result to the first transition line, which extends from point $x = L$, $t = 0$ to point $x = 0$, $t = L/c$, Fig. 12.

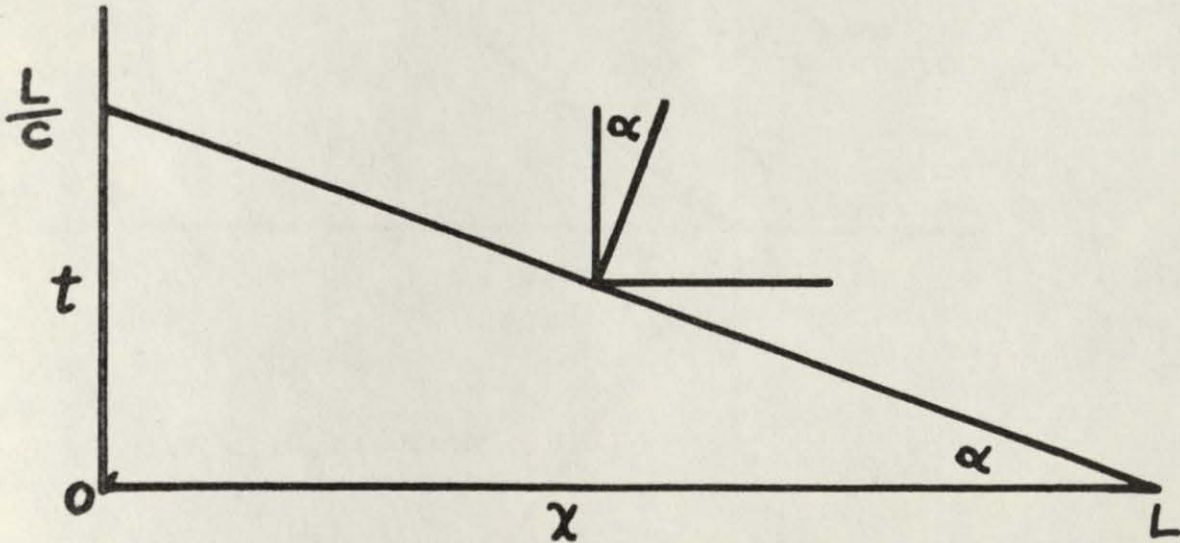


Fig. 12 Application of cylindrical-surface approximation to a transition line.

Here t and x play the roles of ξ and η , respectively; and we consider the slanting plane to be approximated arbitrarily closely by a cylindrical surface in the immediate vicinity of the transition line, as indicated by the edge view Fig. 13.

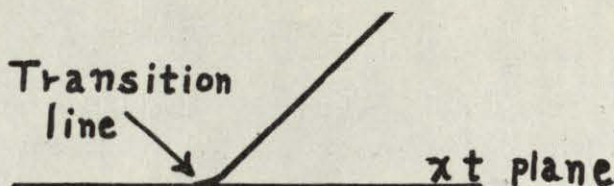


Fig. 13 - Intersection of cylindrical surface with the x, t plane

Equation (103) now gives

$$\frac{\partial^2 s}{\partial x^2} = \frac{\partial^2 s}{\partial t^2} \tan^2 \alpha. \quad (104)$$

Considering the first integration in the double integral in (60), we have seen that the integral

$$\int_0^t \frac{\partial^2 s}{\partial x^2} dt \quad (105)$$

receives contributions only at the transition lines. It is hence zero up to the first transition line. In the vicinity of this line we substitute (104) in (105), and obtain

$$\tan^2 \alpha \int \frac{\partial^2 s}{\partial t^2} dt = \tan^2 \alpha \Delta \frac{\partial s}{\partial t} \quad (106)$$

where the integral extends only from one side of the line to the other. Here $\Delta (\partial s / \partial t)$ is the increment in $\partial s / \partial t$ at the first transition line and $\tan^2 \alpha \Delta (\partial s / \partial t)$ is the corresponding contribution to the integral (105). From (90) and Fig. 10 we see that this increment is

$$v_0 - 0 = v_0; \quad (107)$$

also, from Fig. 12 we see that

$$\tan \alpha = \frac{1}{c}. \quad (108)$$

Substituting in (106) we obtain

$$\left. \begin{aligned} \int_0^t \frac{\partial^2 s}{\partial x^2} dt &= 0 \text{ if } t < t_1 \\ &= \frac{v_0}{c^2} \text{ if } t_1 < t < t_2 \end{aligned} \right\} \quad (109)$$

where, for any value of x , t_1 and t_2 are the values of t for the first and second transition lines, respectively. It follows that

$$c^2 \int_0^t \int_0^t \frac{\partial^2 s}{\partial x^2} dt dt = v_0 (t - t_1). \quad (110)$$

Since $g(x) = 0$ if $x < L$ it follows that for $x < L$ the first term on the right hand side of (60) contributes nothing, s being given entirely by (110), thus

$$s = v_0 (t - t_1). \quad (111)$$

Now t_1 depends upon x , and this expression is evidently in accord with the results shown in Fig. 10. The behavior of the double integral at the succeeding transition lines can be obtained in a similar manner.

Simplification of the Integral Equation. Dividing by Lv_0 , the integral equation (60) may be written

$$\frac{s}{Lv_0} = \frac{ct}{L} \frac{g(x)}{cv_0} + \frac{c^2}{Lv_0} \int_0^t \int_0^t \frac{\partial^2 s}{\partial x^2} dt dt. \quad (112)$$

Placing

$$\frac{s}{Lv_0} = \bar{s}, \quad \frac{ct}{L} = \bar{t}, \quad \frac{x}{L} = \bar{x}, \quad \frac{g(x)}{cv_0} = \bar{g}(\bar{x}), \quad (113)$$

(112) becomes

$$\bar{s} = \bar{t} \bar{g}(\bar{x}) + \int_0^{\bar{t}} \int_0^{\bar{t}} \frac{\partial^2 \bar{s}}{\partial \bar{x}^2} d\bar{t} d\bar{t}. \quad (114)$$

But this integral equation is identical with that obtained by placing

$$L = 1, \quad c = 1, \quad v_0 = 1 \quad (115)$$

in (60). It follows that in devising approximate methods of solution we need only consider this special case, since by using (113) the results so obtained can be applied to any case.

Numerical Integration Scheme. The first question which arises is what formulas to choose for numerical differentiation and integration. In order to keep the individual steps as simple as possible let us, at least temporarily, choose the trapezoidal formula for integration, and the three point differentiation formula based on the quadratic polynomial. We thus have

$$\int_a^{a+nh} f(x)dx \cong h \left[\frac{1}{2} f(a) + f(a+h) + f(a+2h) + \dots \right. \\ \left. + f(a+[n-1]h) + \frac{1}{2} f(a+nh) \right], \quad (116)$$

$$f''(x) \cong \frac{1}{h^2} [f(x-h) - 2f(x) + f(x+h)], \quad (117)$$

where h is the equal spacing between adjacent points. Accuracy will be achieved by having a sufficiently small spacing rather than by using more elaborate formulas for differentiation and integration.

Taking advantage of (115) we shall place $L = 1$, $c = 1$, $v_0 = 1$; also

$$\left. \begin{aligned} g(x) &= 0 \text{ if } 0 \leq x < 1, \\ g(x) &= 1 \text{ if } x = 1. \end{aligned} \right\} \quad (118)$$

Since there is no danger of ambiguity we shall omit the bars on s , t , x , and g ; however, (113) can be used at any time to convert any given problem to that which we are now considering. Figure 9 now becomes Fig. 14. On this figure the values of $\partial s / \partial x$ and $\partial s / \partial t$ on the various component plane surfaces are labeled, these values being given by (88), (89), (90), and (91). For convenience we shall use the same spacing h in both x and t , the result being a square lattice in the xt plane, Fig. 14. Later some preliminary calculations will be made with $h = .05$; however, for the present let us

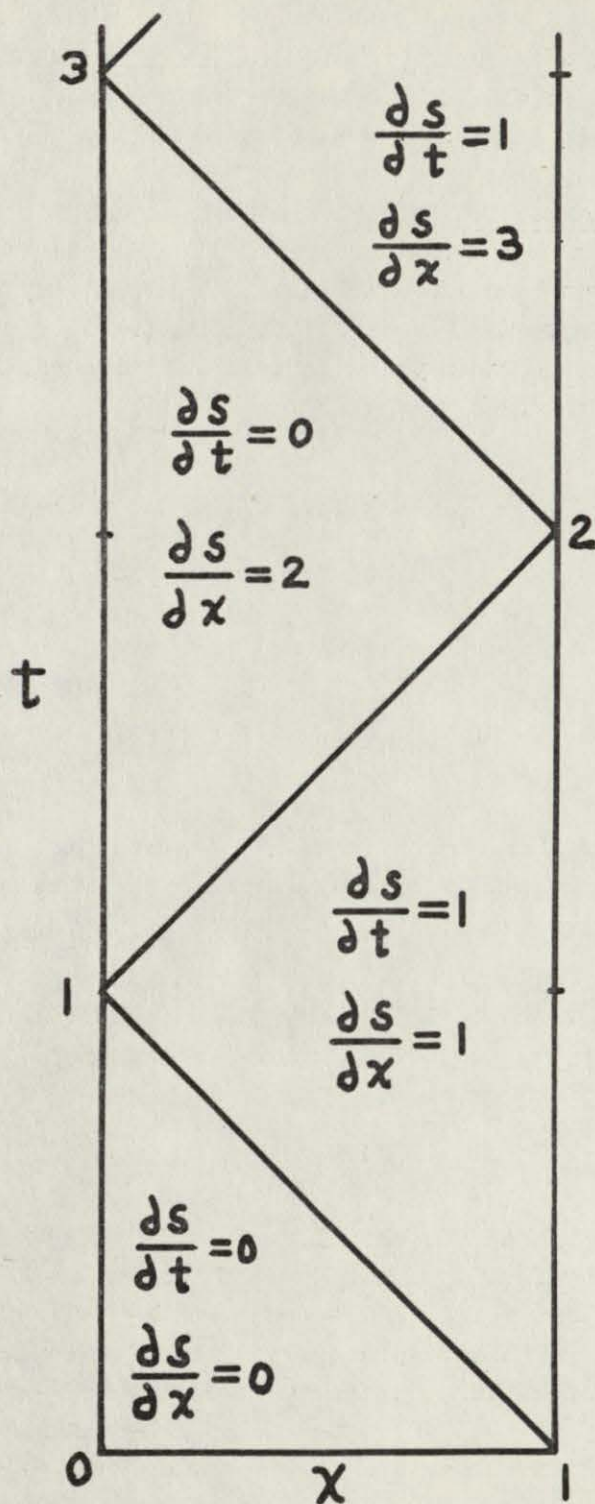


Fig. 14 Top view of the $s(x,t)$ surface with variables normalized. Values of $\partial s/\partial t$ and $\partial s/\partial x$ are shown for the various regions; the values change abruptly at the transition lines.

suppose that h is chosen arbitrarily, then fixed. On the boundaries

$$\left. \begin{aligned} s &= 0 \text{ on the } x\text{-axis and } t\text{-axis,} \\ s &= t \text{ on the line } x = 1. \end{aligned} \right\} \quad (119)$$

Since $g(x) = 0$ if $x < 1$ our integral equation (114) becomes

$$s = \int_0^t \int_0^t \frac{\partial^2 s}{\partial x^2} dt dt. \quad (120)$$

In the integral equation (120) we see from (117) that the integrand contains a factor $1/h^2$; however, each of the two integrations using (116) introduces a factor h , the result being that h disappears entirely from the integral equation. We are therefore justified in replacing h by 1 in our calculations. Of course n , the number of subintervals in the unit length of string, is still determined by the actual value of h .

In carrying out each repetition of the successive substitution process it would, of course, be possible to cover the entire xt plane $0 \leq x \leq 1$, $0 \leq t \leq T$, where T is the greatest value of t in which we are interested. However, since for the larger values of t the intermediate solutions may fluctuate wildly, there appears to be no point in calculating them for values of t which appreciably exceed that for which the solution has converged. In fact we have everything to gain and nothing to lose by finishing the repetitions for one value of t before proceeding to the next. The intermediate solution obtained is hence that for a single row of lattice points corresponding to a constant value of t . Let us place

$$\left. \begin{aligned} s_{ij} &= s(ih, jh) & i &= 1, 2, \dots, n; \\ & & j &= 1, 2, \dots; \\ & & n &= 1/h. \end{aligned} \right\} \quad (121)$$

Then the successive substitution process is first applied to determine $s_{11}, s_{21}, \dots, s_{n-1,1}$, which lie in the same horizontal row; when this row is finished it is applied to determine $s_{12}, s_{22}, \dots, s_{n-1,2}$; and so on. We note that

$$\left. \begin{aligned} s_{ij} &= 0 \text{ if } i = 0 \text{ or } j = 0, \\ s_{nj} &= jh. \end{aligned} \right\} \quad (122)$$

7. Preliminary Investigations.

Before beginning a program of numerical calculation several things were done by way of preliminary investigation in order to test the convergence, accuracy, and feasibility of the successive substitution process. These will now be described briefly. Only a few of the more significant results of the feasibility studies will be presented in the present report. All of the results, comprising mathematical developments, tables, and curves, are available in reference [9].

Use of the Exact Solution as the First Approximation. First, as a preliminary check the exact solution $s(x,t)$ was chosen to start the successive substitution process, and the result of one cycle of this process was calculated. Referring to the oblique lines in Fig. 14 as "transition lines", and the bands composed of points which lie within a distance $h\sqrt{2}$ of these lines as "transition bands", it was shown that if one cycle of the successive substitution process be carried out starting with the exact solution, the approximate solution obtained differs from the exact solution only in the transition bands, in which it is rounded off somewhat when compared with the sharp corners at the transition lines of the exact solution. The width of a transition band is $h\sqrt{2}$, and is hence a measure of the spacing in the lattice.

It was thus shown that one cycle of the successive substitution process does not lead to a wild result, but to a highly satisfactory one. Another repetition of this cycle would probably result in a further rounding off of the corners; however, this investigation was not pursued further.

Determination of the Solution by Difference Equations. In the case of the present linear problem it is possible to determine the solution toward which the successive substitution process converges using difference equations. The solution of the difference equations gives exactly the values toward which the successive substitution process converges, provided the difference equations and the substitution process are both based on the same lattice spacing. These common values differ somewhat from the exact solution, of course. A comparison between the solution of the difference equations and the results of the successive substitution process is practical for the first few rows of the lattice. The comparison is made one row at a time.

In the case of the first row it follows from (116), (117), (120), and (122) that the final solution satisfies the relations

$$\left(\frac{1}{2}\right)\left(\frac{1}{2}\right)(s_{i-1,1} - 2s_{i1} + s_{i+1,1}) = s_{i1} \quad (123)$$

$$s_{i-1,1} - 6s_{i1} + s_{i+1,1} = 0. \quad (124)$$

This is a second order linear difference equation with constant coefficients, which was solved by the usual procedure for handling such equations.

Not only the quantities s_{i1} , which compose the first row, but the quantities s_{ij} , which compose the j^{th} row, can be determined by a difference equation. This equation is

$$\begin{aligned} & s_{i+1,j} - 6s_{ij} + s_{i-1,j} \\ & = -4 \sum_{k=1}^{j-1} (j-k) (s_{i+1,k} - 2s_{ik} + s_{i-1,k}), \end{aligned} \quad (125)$$

which is also a second order linear difference equation with constant coefficients. Quantities pertaining to the first $(j-1)$ rows are at this point known. This equation was also solved by the usual methods. We note that the above difference equations have nothing in common with those obtained by replacing the partial derivatives in (48) by their difference approximations.

The values of s_{ij} for the first six rows were calculated by means of the above difference equations. The existence of a solution of the integral equation (120) was thereby established; furthermore, the values of s_{ij} so obtained were available as a standard of comparison to evaluate the results obtained at any stage of the successive approximation procedure—at least for $j = 1, 2, \dots, 6$. In addition, we could see whether or not the result of the successive substitution process, when sufficiently converged, gave a reasonably good approximation to the exact solution. From Fig. 15 we see that it does; however, we should expect that a much better approximation would be obtained if the motion of the moving end did not have a discontinuity in velocity, but were more realistic. As things are, the

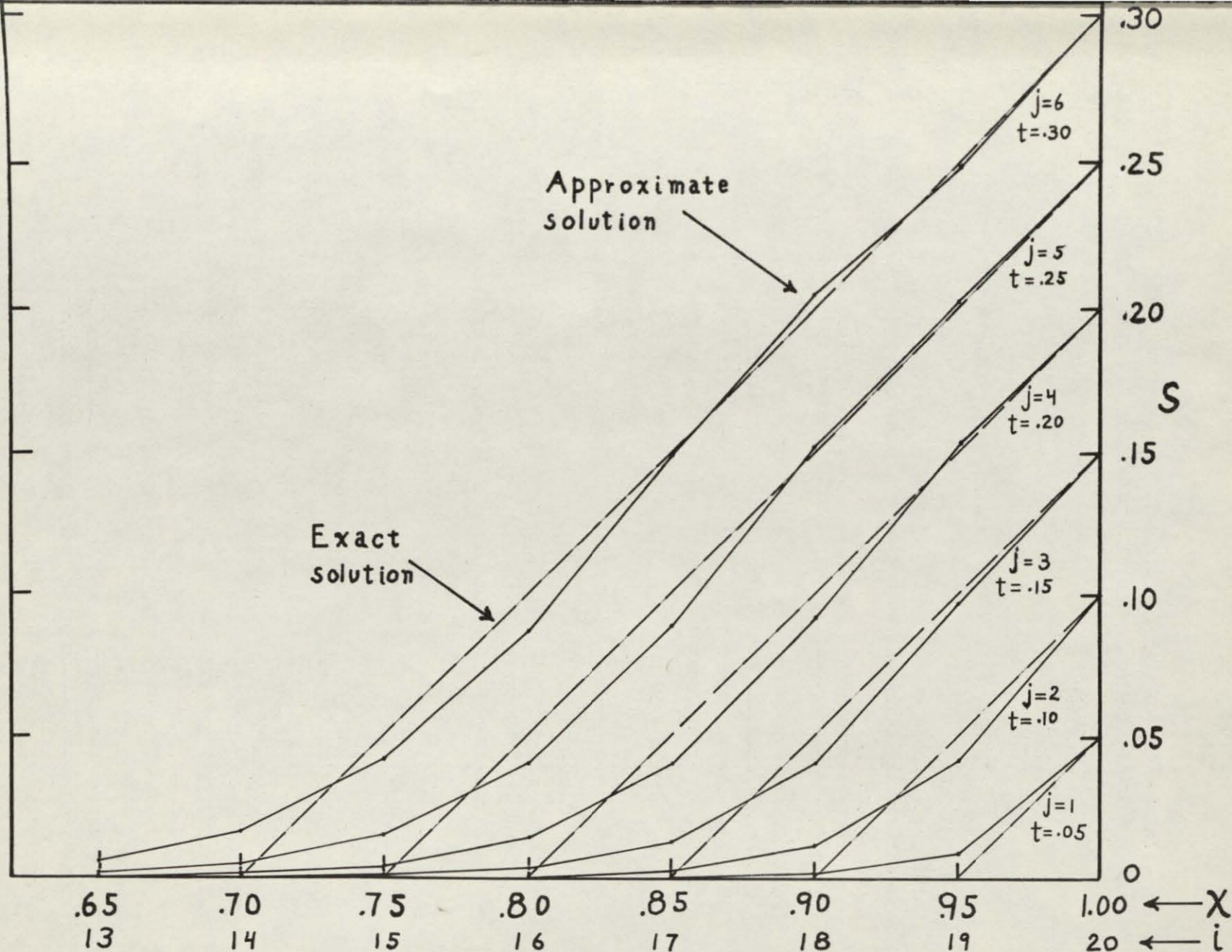


Fig. 15 Comparison between the approximate (successive substitution) solution and the exact solution, for $n = 20$ and $j = 1$ to 6 ($t = .05$ to $.25$). The approximate solution agreed exactly with the solution of the difference equations, which showed that the successive substitution process had converged.

approximate solution is trying to follow the corners which appear in the graph of the exact solution.

8. Preliminary Calculations.

Various preliminary calculations were carried out as follows, using a ten bank desk calculator.

A. Calculation of s_{i1} by Successive Substitutions. Sixteen repetitions of the successive substitution process for determining s_{i1} , the values of s_{ij} for the first row, were carried out. The results obtained for $i = 19$ and 18 are plotted as solid lines in Fig. 16. Note that $n = 20$ and that the plotted results refer to the two lattice points immediately adjacent to the moving end of the string. The values plotted are those resulting from the $(k-1)^{\text{th}}$ repetition, these being used to begin the k^{th} repetition. The dotted and dashed lines in the figure refer to modifications of the successive substitution method, made in attempts to speed up convergence. These will be discussed later.

In determining the displacements (s_{i1}) in the first row, we may expect convergence first for the higher values of i such as $i = 19$ or 18 that are near the given value $s_{20,1}$. Only after convergence in this region is well on the road can we expect convergence for lower values of i ; and such, indeed, is the case.

The values of s_{i1} obtained after sixteen repetitions were compared with the exact values, which are known. It appears that the process is converging; however, at this point values of s_{i1} for $i < 17$ have not yet really begun to settle down.

B. Application of the Successive Substitution Process to the Results Obtained for the First Row ($j=1$) by the Difference Equation Method.

Starting with the values s_{i1} obtained by the difference equation method for $i = 9, 10, \dots, 19$, one cycle of the successive substitution process was carried out to obtain values of s_{i1} for $i = 10, 11, \dots, 19$. These were compared with the original values, and it was found that to the capacity of the machine the output of the process duplicates the input. This provides an independent check on the values obtained by the difference equation method; also it illustrates the

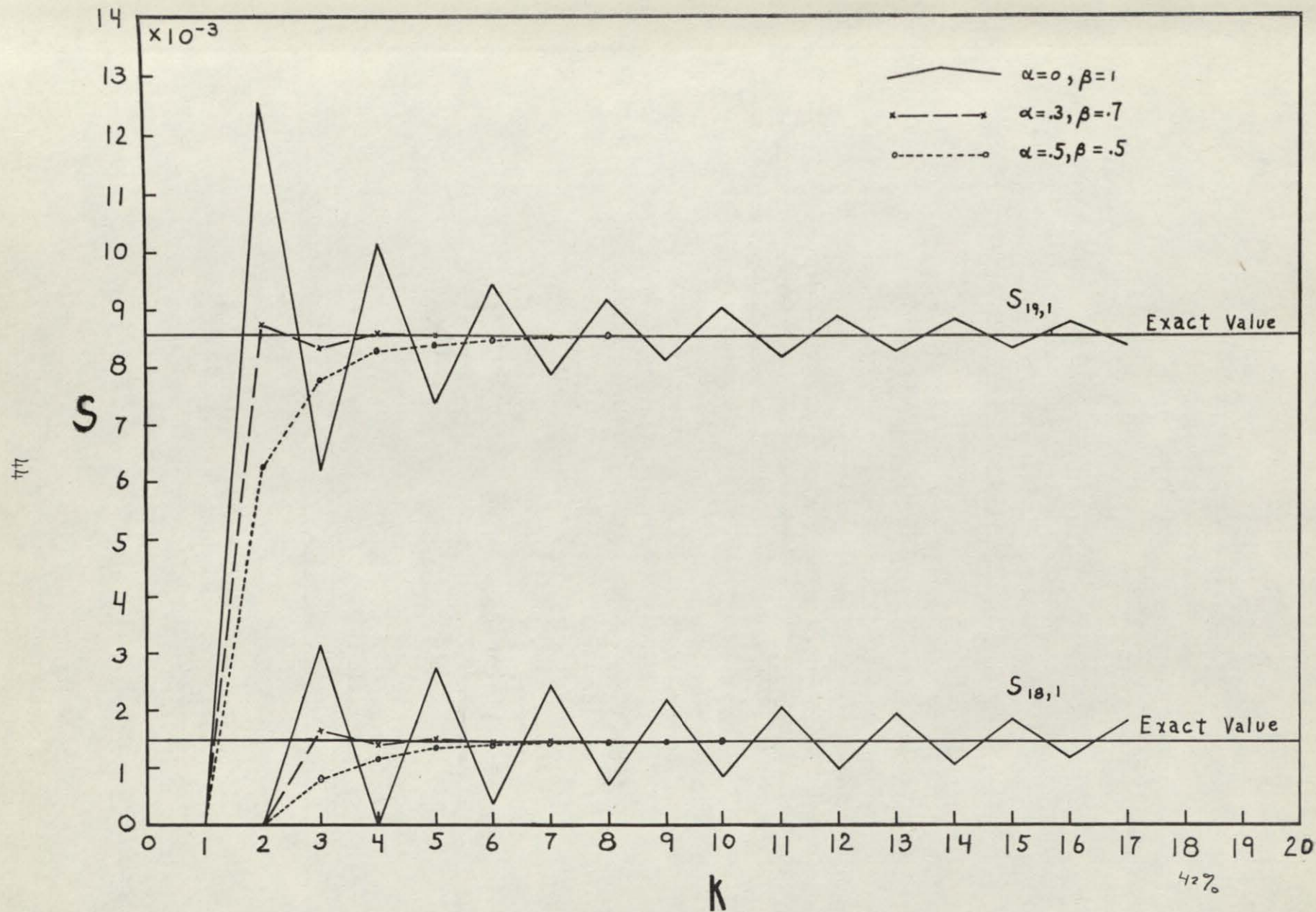


Fig. 16 Convergence of s -values at two selected lattice points in the first row. Solid line, unmodified procedure; other lines, modified output taken as $\alpha \times$ input + β unmodified output.

last step which would have been taken in Part A if the successive substitution process had been carried to completion.

C. Calculation of s_{i1} Using a Weighting Factor of .3 with the Input and .7 with the Output. As we examine Fig. 16 we note that the convergence obtained is of the nature of a damped oscillation - the successive calculated values overshoot the true value. In view of this it appears that the true value would be more closely approximated by an average of the values obtained after two consecutive repetitions of the successive substitution process than by the value obtained last. The procedure used so far may be shown schematically by the diagram Fig. 17.

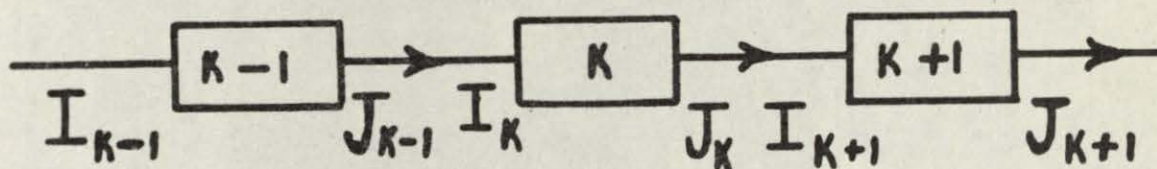


Fig. 17 Schematic representation of successive substitution process.

Here the blocks represent the various repetitions, I_k is the input to the k^{th} repetition and J_k is the output of the k^{th} repetition. In the process which we have been using

$$J_k = I_{k+1}$$

To increase the damping of the oscillation the output of one stage can be coupled to that of the preceding stage, as indicated by Fig. 18, and described by the relation

$$\alpha J_{k-1} + \beta J_k = I_{k+1} \quad (126)$$

where the weighting factors α and β are constant, are chosen once and for all, and satisfy the relation

$$\alpha + \beta = 1. \quad (127)$$

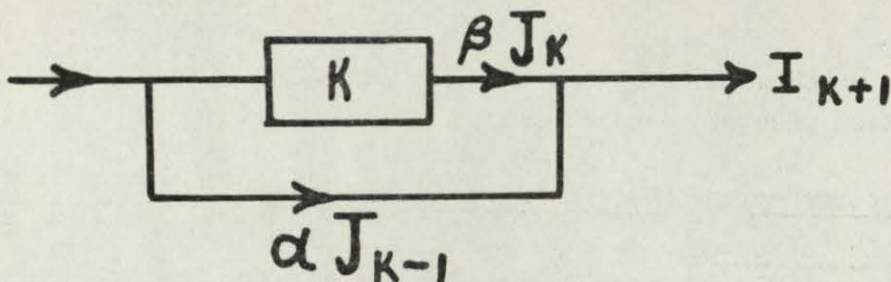


Fig. 18 Schematic representation of one step in modified substitution process, in which the weighting factors α and β are used.

In choosing α and β a number of factors are evident as follows.

1. If $\alpha = 1$, $\beta = 0$ the k^{th} repetition has no effect; hence we require that $\alpha < 1$, $\beta > 0$.
2. If convergence is achieved through a damped oscillation when $\alpha = 0$, $\beta = 1$, the damping or rate of convergence will be improved if β is reduced from unity to some value which exceeds .5 (see Fig. 16).
3. If convergence is achieved without oscillation by approaching the limit from one side when $\alpha = 0$, $\beta = 1$, the rate of convergence will be improved if β is increased from unity to as large a value as can be used without causing overshooting and hence oscillation.
4. Since the requirements of 2. and 3. are contradictory, and since in any case we do not know whether or not the convergence is achieved through a damped oscillation, we should choose a value of between .5 and 1 which is small enough to greatly help the convergence if oscillation is involved, but not so small as to greatly hurt the convergence if oscillation is not involved. Of the possible choices $\beta = .5, .6, .7, .8, .9$, we can rule out .5 as being smaller than we need or want, and .9 as not differing enough from unity. If there is oscillation, $\beta = .6$ is very likely a good value, but .7 should be almost as good when oscillation is present and appreciably better if there is no oscillation. We could put $\beta = .8$ but this seems a little close to unity. All in all, it appears that the best value we can choose in the absence of any

data is $\beta = .7$. We shall hence tentatively place

$$\alpha = .3, \beta = .7. \quad (128)$$

We now have two ways in which intermediate results are improved, as follows.

- a) The carrying out of a repetition of the successive substitution process.
- b) The calculation of the weighted average (126) to give I_{k+1} .

At this point Robert Crout* suggested that since the weighted average I_k is better than the preceding output J_{k-1} , the latter should be discarded in favor of the former in subsequent calculations, in particular, this should apply to (126). This suggestion seems reasonable; hence we shall supersede (126) by the relation

$$\alpha I_k + \beta J_k = I_{k+1} \quad (129)$$

The considerations which led to the choice $\alpha = .3, \beta = .7$ remain unaltered; hence we shall tentatively retain (128).

Since the calculation of the weighted average b) is much easier than the carrying out of a repetition a), and does lead to an improvement in the results, it was suggested by Robert Crout that where the process of successive repetitions is terminated before convergence has been achieved the last step be of the type b). This is equivalent to regarding the result obtained after the k^{th} repetition to be I_{k+1} instead of J_k . This suggestion seemed reasonable, and was followed.

Equations (128) and (129) together give

$$.3I_k + .7J_k = I_{k+1}. \quad (130)$$

*Robert Crout made many of the preliminary calculations of the present investigation on a desk calculator, under the direction of his father, Prescott D. Crout.

Fourteen successive repetitions based on (130) were carried out. The results after the various repetitions are shown for $s_{19,1}$ and $s_{18,1}$ in Fig. 16. We see that the present method of successive repetitions of the process based on (130) is very much better and leads to much more rapid convergence than does the unmodified successive substitution process considered in Part A.

Finally, it may be mentioned that we should expect to obtain convergence using any value of β lying in the range $0 < \beta \leq 1$; however, as we have seen, the rate of convergence depends upon the value chosen.

D. Calculation of s_{ij} Using a Weighting Factor of .5 with the Input and .5 with the Output. Fourteen repetitions were carried out in computation of s_{11} with $\alpha = .5$, $\beta = .5$. The resulting convergence of $s_{19,1}$ and $s_{18,1}$ are shown in Fig. 16. We note that the convergence is not oscillatory. We have seen that reducing β increases the damping of an oscillation.

Comparing the results of parts C and D we see that the convergence is better with $\alpha = .3$, $\beta = .7$ than it is for $\alpha = .5$, $\beta = .5$. The latter values are little, if any, better than the former in the case of oscillation, and are appreciably worse if there is no oscillation.

E. Calculation of s_{i6} Using Successive Substitutions. We have just finished considering the determination of the first row s_{11} . There is no reason to make preliminary calculations on more than one additional row; hence let us proceed directly to the determination of the sixth row, since that is the last for which we have calculated exact values of s_{ij} , in this case s_{i6} , using the difference equation method.

We shall first use the method of successive substitutions ($\alpha = 0$, $\beta = 1$), and shall consider the exact values of s_{ij} for the first five rows to be given. To start the process, values of s_{i5} in the fifth row, which are known, are taken as the first approximation to the corresponding values of s_{i6} . Fourteen repetitions were carried out, the resulting convergence of $s_{19,6}$ and $s_{18,6}$ being shown in Fig. 19 (solid lines). In this figure it should be noted that the origin is not shown. The repetition number is $(k-1)$.

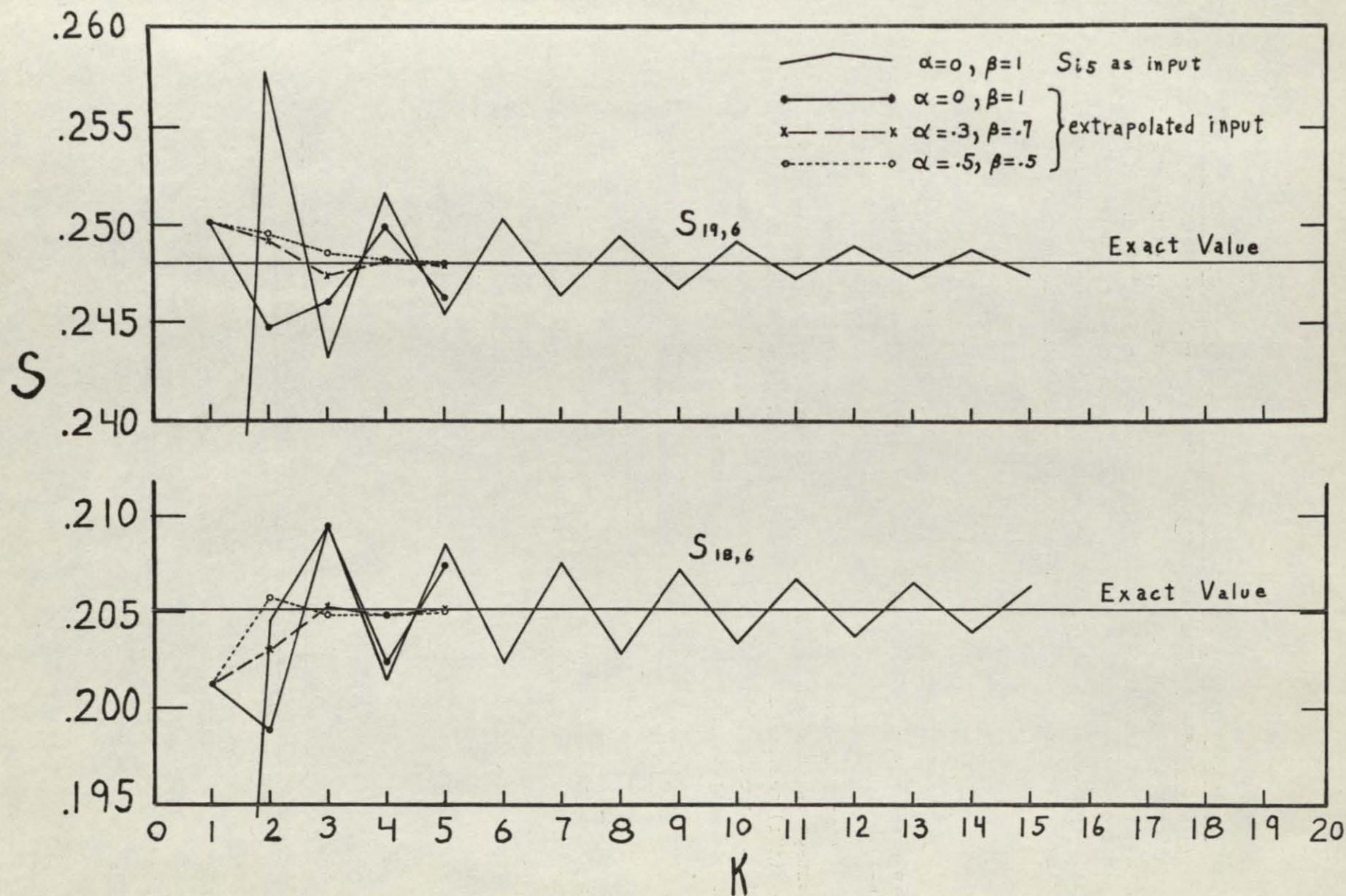


Fig. 19 Convergence of s -values at two selected lattice points in the sixth row. The use of an extrapolated input is compared with the use of the values in the preceding row. Also, the effect of using weighting factors is shown.

F. Calculation of s_{16} Using Successive Substitutions Starting with Values Obtained by Extrapolation. The present calculations differ from those in Part E only in that more accurate initial values are used to start the successive substitution process. Whereas in Part E s_{15} is taken as the first approximation to s_{16} , we shall now take as the first approximation to s_{16} the value obtained by linear extrapolation using s_{14} and s_{15} . We thus have as our first approximation

$$s_{16} = s_{15} + (s_{15} - s_{14}) = 2s_{15} - s_{14}. \quad (131)$$

Four repetitions are carried out, the resulting convergence of $s_{19,6}$ and $s_{18,6}$ being shown in Fig. 19. The repetition number is $(k-1)$.

Comparing these last two results, it appears that whatever advantage is obtained by using the more accurate initial values given by (131) can be achieved more easily by using the values of s_{15} as first approximations to the values of s_{16} and using two or three more repetitions of the iterative process.

G. Calculation of s_{16} Using a Weighting Factor of .3 with the Input and .7 with the Output, and Starting with Values Obtained by Extrapolation. Four repetitions were carried out using a weighting factor of .3 with the input and .7 with the output ($\alpha = .3$, $\beta = .7$). The first approximation was obtained by linear extrapolation using (131). We have already seen in section F that the linear extrapolation is not worth the trouble but now we wish to see the advantage of using various weighting factors. The convergence of $s_{19,6}$ and $s_{18,6}$ with $\alpha = .3$ and $\beta = .7$ is shown in Fig. 19. We see that the convergence is very much improved by the use of weighting factors, as compared with the convergence obtained in Parts E and F using the method of successive substitutions ($\alpha = 0$, $\beta = 1$).

H. Calculation of s_{16} Using a Weighting Factor of .5 with the Input and .5 with the Output, and Starting with Values Obtained by Extrapolation. Four repetitions were carried out using a weighting factor of .5 with the input and .5 with the output ($\alpha = .5$, $\beta = .5$). The first approximation was obtained as in F and G by linear extrapolation using (131). The resulting convergence of $s_{19,6}$ and $s_{18,6}$ is shown in Fig. 19. Comparing the results in Fig. 19 we see that for $s_{19,6}$ and $s_{18,6}$ there is not much difference in convergence rates

when $\alpha = .3$, $\beta = .7$ and when $\alpha = .5$, $\beta = .5$. However, both sets of weighting factors give much more rapid convergence than the unmodified process that corresponds to $\alpha = 0$, $\beta = 1$, and we recall that $s_{19,1}$ and $s_{18,1}$ converged most rapidly when $\alpha = .3$, $\beta = .7$. As a consequence of the above preliminary calculations we have found that:

1. The convergence of the successive substitution process is for all practical purposes established.
2. The rate of convergence is very greatly improved by using weighting factors, as described on page 47.
3. On the basis of the work done so far the recommended values of the weighting factors are $\alpha = .3$ and $\beta = .7$, which lead to the fundamental relation (130).
4. The use of linear extrapolation using (131) to obtain the first approximation is not worthwhile, since the improvement which it gives can more easily be achieved by a few more repetitions. It is recommended that the known values $s_{i,j-1}$ be taken as the first approximation of the corresponding values s_{ij} .

The above recommendations are incorporated in the following set of instructions for programming the successive repetition process for use in connection with a digital computer. In these instructions A is a measure of the first time-integral, whereas B is a measure of the second.

9. Description of the Repetitive Process When Applied to the Linear String.

Our problem is to determine the values of the quantity s_{ij} at the points of a square lattice, in which i takes the values $0, 1, 2, 3, \dots, n$; and j takes the values $0, 1, 2, 3, \dots$. Since n is given, the range of values taken by i is bounded. The range of values taken by j , however, has no upper bound except, possibly, one which will be assigned later from practical considerations, Fig. 20.

The values of s_{ij} are given for those points which lie on the border, thus

$$\left. \begin{aligned} s_{0j} &= 0 & j &= 0, 1, 2, 3, \dots; \\ s_{i0} &= 0 & i &= 0, 1, 2, 3, \dots, n; \\ s_{nj} &\text{ is given, } & j &= 0, 1, 2, 3, \dots \end{aligned} \right\} \quad (132)$$

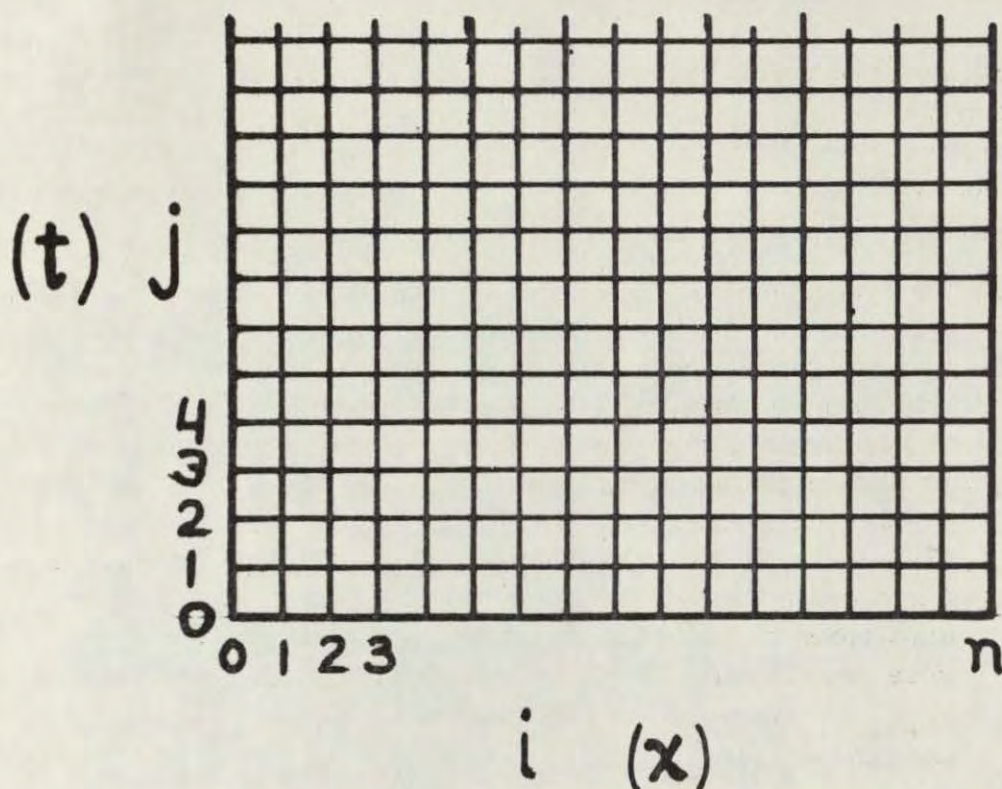


Fig. 20 Lattice of points at which calculations are to be made.

The values of s_{ij} at the other points are determined a row at a time — that is for j fixed and $i = 1, 2, 3, \dots, (n-1)$. The values of j are taken in the order $1, 2, 3, \dots$. In view of this it will evidently be sufficient to describe how to obtain the values of s_{ij} for the j^{th} row when the values for all of the preceding rows are known.

The values of s_{ij} for the j^{th} row are obtained as the limits gotten, respectively, by applying repeatedly a process shortly to be described. At the beginning of the k^{th} repetition we have the quantities

$$s_{1j}^{(k)}, s_{2j}^{(k)}, s_{3j}^{(k)}, \dots, s_{n-1,j}^{(k)} \quad (133)$$

as approximations to the quantities

$$s_{1j}, s_{2j}, s_{3j}, \dots, s_{n-1,j} \quad (134)$$

respectively. Here (k) is a superscript, not an exponent. When the process is applied starting with the quantities (133), the quantities

$$s_{1j}^{(k+1)}, s_{2j}^{(k+1)}, s_{3j}^{(k+1)}, \dots, s_{n-1,j}^{(k+1)} \quad (135)$$

are obtained as approximations to (134) respectively. The sequence of repetitions is started by taking the values of s_{ij} for the $(j-1)^{th}$ row as approximations to the values for the j^{th} row, respectively, thus

$$s_{1j}^{(1)} = s_{1,j-1}, s_{2j}^{(1)} = s_{2,j-1}, \dots, s_{n-1,j}^{(1)} = s_{n-1,j-1}. \quad (136)$$

These values are, of course, known. The sequence of repetitions is terminated when, for sufficiently large k , the output (135) duplicates the input (133) to the required accuracy. The common values which then compose (133) and (135) are taken as the final result (134). The values of s_{ij} which compose the j^{th} row are thus determined.

Finally, we shall describe the process by which we start with (133) and obtain (135). During the course of the calculations we compute and record, in addition to the quantities s_{ij} , the auxiliary quantities A_{ij} and B_{ij} . These quantities do not exist at the points of the left border of the lattice, for which $i = 0$, or the right border, for which $i = n$. Along the lower border, where $j = 0$, they are defined to be zero, thus

$$A_{10} = 0, A_{20} = 0, A_{30} = 0, \dots, A_{n-1,0} = 0; \quad (137)$$

$$B_{10} = 0, B_{20} = 0, B_{30} = 0, \dots, B_{n-1,0} = 0. \quad (138)$$

As is the case with s_{ij} the auxiliary quantities A_{ij} and B_{ij} are obtained one row at a time, are known in the first $(j-1)$ rows, and are obtained in the j^{th} row as the limits approached by the quantities $A_{ij}^{(k)}$ and $B_{ij}^{(k)}$, respectively, during the course of the successive repetitions. The desired basic process is now described by the

relations

$$A_{ij}^{(k)} = A_{i,j-1} - s_{i,j-1} - s_{ij}^{(k)} + \frac{1}{2} (s_{i-1,j-1} + s_{i+1,j-1} + s_{i-1,j}^{(k)} + s_{i+1,j}^{(k)}), \quad i = 1, 2, \dots, (n-1); \quad (139)$$

$$B_{ij}^{(k)} = B_{i,j-1} + \frac{1}{2} (A_{i,j-1} + A_{ij}^{(k)}), \quad i = 1, 2, \dots, (n-1); \quad (140)$$

$$s_{ij}^{(k+1)} = .3 s_{ij}^{(k)} + .7 B_{ij}^{(k)}, \quad i = 1, 2, \dots, (n-1). \quad (141)$$

Starting with the given quantities $s_{ij}^{(k)}$, j being fixed and i taking the values $1, 2, \dots, (n-1)$, we compute the quantities $A_{ij}^{(k)}$ using (139); then the quantities $B_{ij}^{(k)}$ using (140); and finally the quantities $s_{ij}^{(k+1)}$ using (141). This process is now repeated until all values of s_{ij} have adequately converged. Row $j+1$ is then computed in a similar manner and the calculation of successive rows is continued until the time range of the problem has been covered.

10. Typical Results Obtained by Digital Computer, Using the New Methods.

The preceding analysis has dealt with the problem of a linear string, one end of which is instantaneously set in motion with constant velocity at time 0. A computer program applying the successive-substitution method to this problem was written and tested out. Putting $n = 20$, the computed results should agree exactly with the solution of the finite-difference equations shown in Fig. 15; this, in fact, they did. But whereas with the finite difference equations and the desk calculator it was impractical to go much beyond $n = 20$ and $j = 6$, the high-speed computer could easily handle $n = 100$, with j ranging up to 300 or even higher.

Figure 21 shows displacement s versus x as obtained by computer, with $n = 100$, for two typical rows of computer output, for which $j = 75$ and $j = 275$, respectively. The computed quantities are normalized according to equations (114) to (117); unit strain travels with unit velocity in a string of unit length. Hence the first curve ($j = 75$), corresponds to $t = .75$, when the wave front has traveled

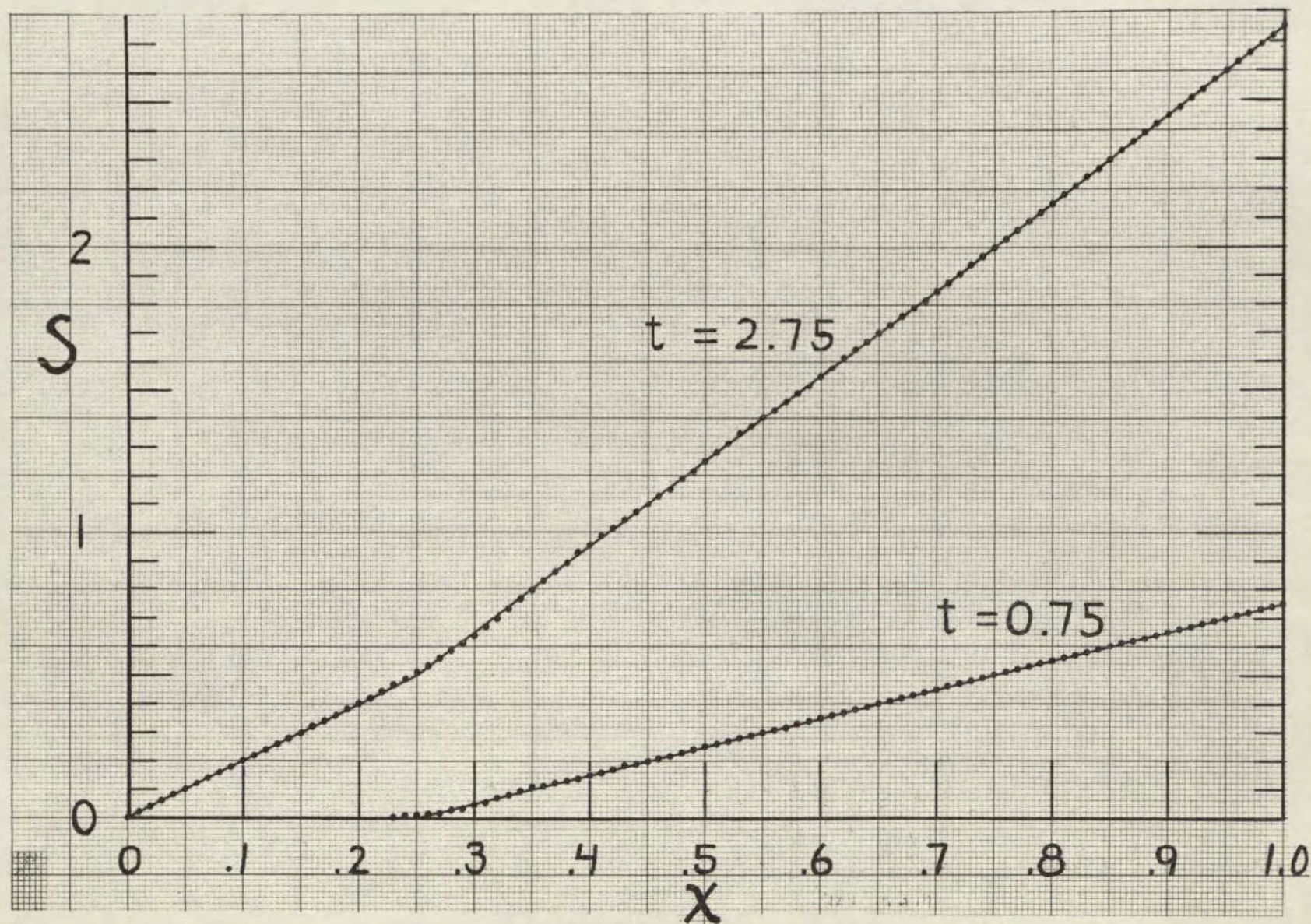


Fig. 21 Values of s calculated by digital computer with $n = 100$. The lower curve is for $j = 75$ ($t = .75$) and the upper is for $j = 275$ ($t = 2.75$).

$3/4$ the length of the string. The second curve ($j = 275$) corresponds to $t = 2.75$, when the wave front has been reflected twice and has completed $3/4$ of its third passage. The exact solution of this problem is known to consist of two straight lines having a corner (discontinuity in slope) at the position of the wave front. The differences between the computer solution and the exact solution are hardly noticeable although on a large-scale graph it can be seen that the computer solution oscillates from side to side of the exact solution.

In addition to the displacement s it is almost always desirable to compute the strain $\epsilon = \partial s / \partial x$. Differences between experimentally observed and calculated strains are more convenient to compare than the corresponding differences in displacements. Although appearing in the basic differential and integral equations, the strain does not appear explicitly in the program for the linear string where approximate formulas are used. Rather the quantities from which the strain could be calculated are to be found. However, in later programs various quantities are functions of strain and also strain values are required for comparison with other calculations and experimental results. Therefore the strain results for this problem should be examined. They were calculated by hand from a simple two point formula,

$$\epsilon_{i-1/2,j} = n (s_{i,j} - s_{i-1,j}).$$

(Practically the same results were obtained with a five point formula.)

Figure 22 shows strain plotted against x for the same times as in Fig. 21. The exact solution is shown by the horizontal and vertical straight lines. In this figure the departures of the computer solution from the exact solution are very much more noticeable than they were in Fig. 21. This is to be expected, since the ordinates in Fig. 22 are the slopes of the corresponding curves in Fig. 21. The oscillations of the computer solution undoubtedly originate because a finite-difference method cannot conform exactly to the sudden discontinuity in strain at the wave front. In the computer solution the wave front has a finite slope whereas the true slope is infinite. In the computer solution the strain does not reach its full value when the exact solution does, but lags behind. When the computer solution does reach the true value it overshoots. The

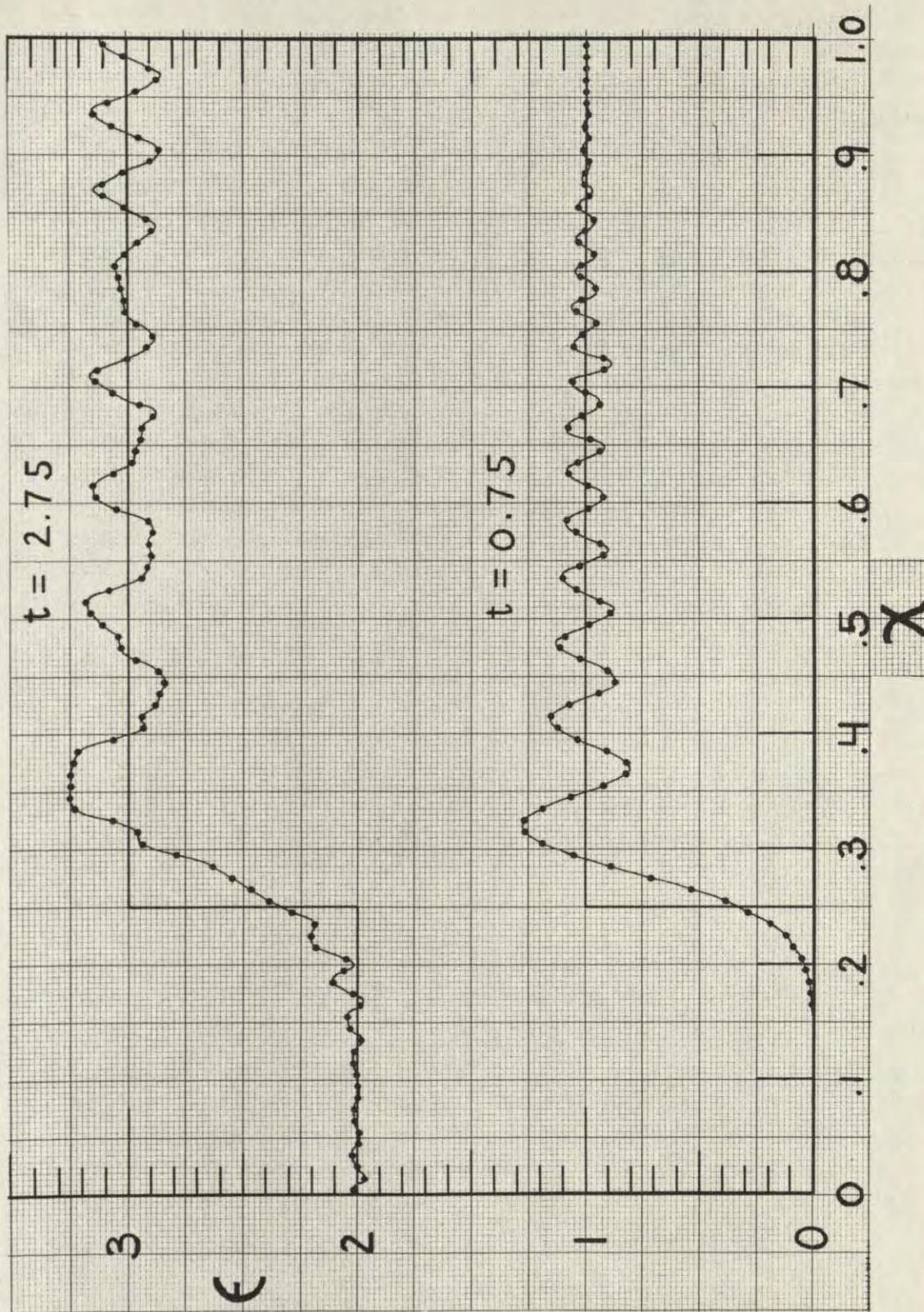


Fig. 22 Values of strain (ϵ) taken from the computer data of Fig. 21.

overshooting is eventually corrected but the correction is too large and causes undershooting. The result is that the computer solution oscillates back and forth across the line representing the exact solution.

The oscillations of the computer solution above and below the exact solution in Fig. 22 are larger than we would like. Therefore, it is an important point that in practical problems factors are present that will reduce the amplitude of the oscillations. To see that nonlinearity of the stress-strain curve can be beneficial in this respect, we note that in a non-linear material the velocity of strain propagation depends on the level of strain. In the usual case small strains travel more rapidly than large strains. In such a case a large strain consists of a rapidly moving leading edge followed by a slower-moving crest; the strain rises gradually as the wave-front passes, not discontinuously. The slope of the front becomes more and more gradual as the wave travels, and solutions computed by the method of successive substitutions can conform more and more closely to it. If a square wave were ever present in such a case it would rapidly deform into a wave with a slanting front.

Situations can arise, in theory at least, (when the stress-strain curve is concave upward) in which large strains travel more rapidly than small strains. In such a case an initially slanting wave front becomes steeper until a shock wave is formed. Such situations will be encountered later, but only in the computations, not in the experimental data. So far as we are aware, there is no conclusive evidence that shock waves are ever produced in tensile impact experiments. Situations in which the computations lead to shock waves must be excluded when we say that nonlinearity reduces the oscillations in computer solutions; some situations to be treated in a later report indicate that the tendency to form shock waves may aggravate the oscillations in computer solutions.

The effect of time-dependence (creep or recovery) in reducing oscillations in computer solutions should always be favorable. When part of the response of the material is delayed, the shape of a square wave will be distorted as the wave travels, and the distortion will tend to smooth out discontinuities, making it easier for the successive-substitution method to follow the actual strains.

In the exact solutions presented above, which we wish to match

with the computer solution, the acceleration of the moving end of the string occurs in zero time. If we give up this condition, which is actually unrealistic, and allow the end of the string to experience a constant acceleration during a small finite time, the problem is much more easily handled by the new method and the oscillations about the exact solution are much reduced. A single discontinuity in velocity has been replaced by two discontinuities in acceleration. The exact solution for this case can be obtained as described in Appendix A. The computer program for the new boundary condition needs only to be modified by specifying the actual motion.

A computation was made for the case of a finite velocity-rise-time, with the velocity of the impacted end of the string rising linearly from 0 to v_0 , in the time interval 0 to .5. This rise time was typical of what was observed in much of the experimental data. In Fig. 23 the exact and computed solutions for row 105 are compared. The usual square lattice was taken, with $n = 60$, hence $t = 1.75$. The leading edge of the strain wave has travelled 1.75 times the length of the string and the trailing edge has traveled 1.25 times the length of the string. As before, the straight lines represent the exact solution and the curved line represents the computer solution. Comparing Fig. 23 with Fig. 22 we see that the substitution of a continuous rise in velocity for the instantaneous rise has very greatly reduced the tendency of the computer solution to oscillate. Whereas in Fig. 22 the greatest departure of the computer strain from the exact solution was 28 percent, the greatest departure in Fig. 23 is only 3 percent.

In an actual situation the finite rise-time of velocity will help to reduce the errors, due to oscillations, of the successive-substitution computer-solution. Delayed response of the material will also make it easier for oscillations in the computer solution to be avoided. Nonlinearity of the material will generally, but not always, have a salutary effect. All in all, we consider the oscillations of the computer solution to be troublesome but not serious and accept the validity of the computer solution as established.

One might expect the oscillations of the computer solution to decrease as the lattice spacing h is decreased. A test was made, putting $n = 1/h = 20, 40, 60$, and 100, and solving our zero-rise-time problem. Increasing n greatly improves (increases) the steepness of the computed wave front. It reduces the wavelength of the

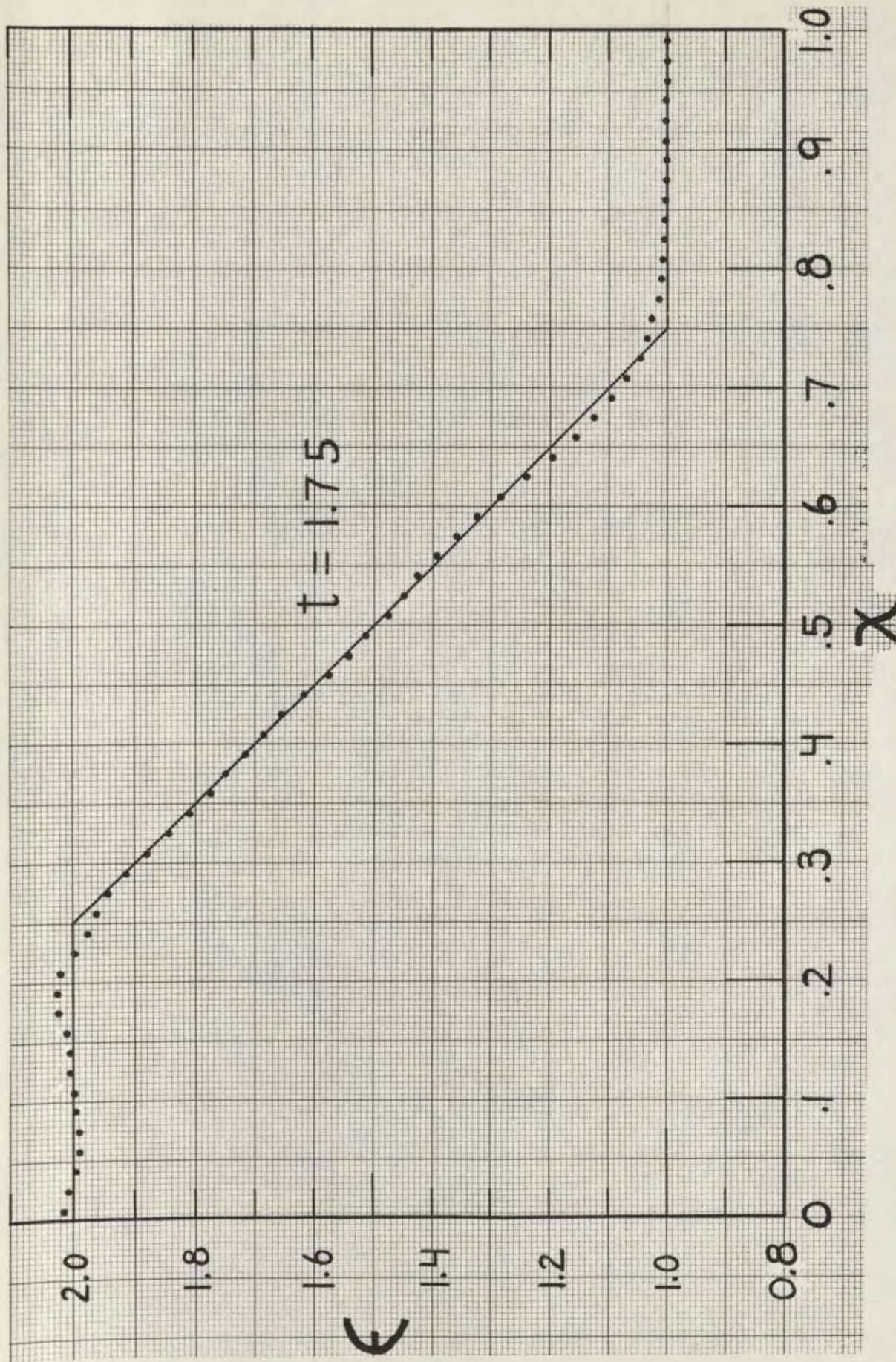


Fig. 23 Strain as obtained from digital computer calculations, for $n = 60$ with $j = 105$ ($t = 1.75$). In earlier graphs the acceleration of the impacted end of the string has occurred in zero time whereas here the acceleration is finite and constant and occurs in the interval

oscillations, but it does not reduce the amplitude of the oscillations as much as might be hoped.

Fortunately, the amplitude of the oscillations in a particular region falls as the wave front travels away from that region. This is shown in Fig. 24. The lower curve ($t = .5$) represents the 50th row of the calculated lattice points. The upper curve ($t = 1.5$) represents the 150th row of the lattice. In the right-hand half of the string there has been in the meantime no change in the exact solution. The successive-substitution process has, however, modified and smoothed the oscillations in this region. The wavelength of the oscillations at the later time is only about half of that at the earlier time. The amplitude of the oscillations in the meantime has been reduced by a factor of 3 or 4. These two isolated samplings of the oscillations do not of course show how the oscillations behave at intermediate times, but it is reasonable to assume that they gradually diminish in size.

A smooth curve faired through the computer solution, but not following the oscillations, would agree with the exact solution everywhere except in the immediate neighborhood of the front of the square wave. As the oscillations diminish with time, the computer solution settles down to agree more and more closely with the exact solution.

This completes the description of the steps taken in devising the integral equation method as a means for solving partial differential equations, in devising the modified method of successive substitutions for solving the integral equations, and in testing the solution obtained against the exact solution in the case of the linear string.

This description will be continued in the second and third reports of this series, in which integral equation methods will be applied to the non-linear and simultaneous partial differential equations which arise in the treatment of strings composed of nonlinear and time-dependent materials.

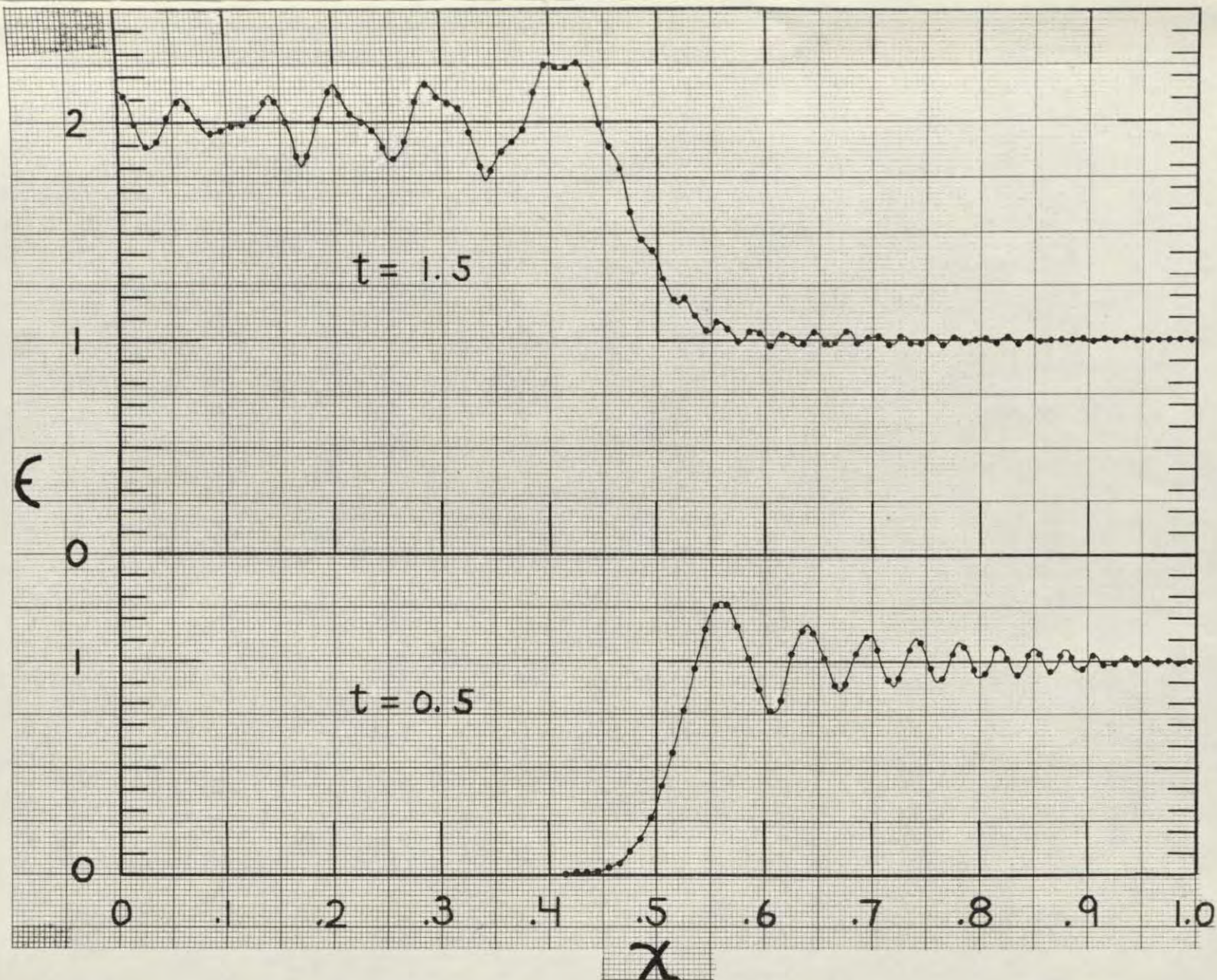


Fig. 24 Strain calculated with $n = 100$, at $n = 50$ ($t = .5$) and $n = 150$ ($t = 1.5$). Note that in the time interval between the two curves, the oscillations in the computer solution have been greatly reduced by the successive-substitution process. Infinite initial acceleration (square wave).

APPENDIX A

Calculation of the Motion of the Linear String When the Motion of the Moving End is Specified Arbitrarily.

In the original treatment the velocity v_0 of the right hand end of the string was considered to be constant. This abrupt change in the end velocity when $t = 0$ gives rise to the corners in the surface $s(x,t)$, as shown in Figs. 9 and 10. These corners in turn were difficult to approximate accurately by the numerical process, and for a given accuracy would require the mesh of the lattice used to be unduly small. Since in an actual experiment the end velocity cannot be changed abruptly it appears that the above difficulty is artificial, and can probably be eliminated if a realistic end-velocity-versus-time function is used instead of a step function. If this is done the numerical procedure is altered only in that s_{nj} is taken from the given motion of the end, and is no longer linear in j . The modification in the numerical process is hence trivial. To test the accuracy of the numerical solution obtained under this new condition it is, as before, desirable to consider a case where the exact solution can be obtained. The linear string provides such a case, as we shall now see.

Referring to (51), which pertains to the linear string, we see that if $s_1(x,t)$ and $s_2(x,t)$ are the solutions obtained, respectively, for the given initial and end conditions

$$\left. \begin{aligned} s(x,0) &= s_1(x,0), \quad \frac{\partial s}{\partial t} \bigg|_{t=0} = \frac{\partial s_1}{\partial t} \bigg|_{t=0} \\ s(0,t) &= s_1(0,t), \quad s(L,t) = s_1(L,t); \end{aligned} \right\} \quad (142)$$

and the conditions

$$\left. \begin{aligned} s(x,0) &= s_2(x,0), \quad \frac{\partial s}{\partial t} \bigg|_{t=0} = \frac{\partial s_2}{\partial t} \bigg|_{t=0}, \\ s(0,t) &= s_2(0,t), \quad s(L,t) = s_2(L,t); \end{aligned} \right\} \quad (143)$$

then the integral equation (51) is satisfied if a subscript 1 be affixed to s wherever it appears. Similarly the integral equation is satisfied if a subscript 2 be so affixed. Adding the two equations so obtained we get

$$\begin{aligned}
s_1 + s_2 = & s_1(x,0) + s_2(x,0) + t \left[\left(\frac{\partial s_1}{\partial t} \right)_{t=0} + \left(\frac{\partial s_2}{\partial t} \right)_{t=0} \right] \\
& + c^2 \int_0^t \int_0^t \frac{\partial^2 (s_1 + s_2)}{\partial t^2} dt dt,
\end{aligned} \tag{144}$$

which equation states that if the two sets of initial and boundary conditions (142) and (143) be superimposed, then the solution is obtained by superimposing the two component solutions $s_1(x,t)$ and $s_2(x,t)$. Superposition is therefore permissible.

In those cases which are of interest to us $s(0,t)$ and $s(x,0)$ both vanish, and $(\partial s / \partial t)_{t=0}$ vanishes if $0 \leq x \leq L$. Our problem is to find $s(x,t)$ when the initial and end conditions are given by

$$\left. \begin{aligned}
s(x,0) &= 0, & 0 \leq x \leq L, \\
s(0,t) &= 0, & 0 \leq t, \\
\left(\frac{\partial s}{\partial t} \right)_{t=0} &= 0, & 0 \leq x < L, \\
\left(\frac{\partial s}{\partial t} \right) &= v_0(t), & x = L.
\end{aligned} \right\} \tag{145}$$

Using superposition let us denote by $s_u(x,t)$ the solution corresponding to (145) with $v_0(t) = 1$ — that is, a step function. The desired function $v_0(t)$ may be regarded to be composed of an infinite number of step functions as indicated in Fig. 25. These start at different times, and our objective is to find their cumulative effect at time t . The elementary step function of magnitude dv_0 which begins at time τ acts during a time $(t-\tau)$, and hence contributes an amount $s_u[x, (t-\tau)] dv_0$ to $s(x,t)$. Since $s(x,t)$ is composed of the sum of such contributions it follows that

$$s(x,t) = \int_0^{v_0(t)} s_u[x, (t-\tau)] dv_0. \tag{146}$$

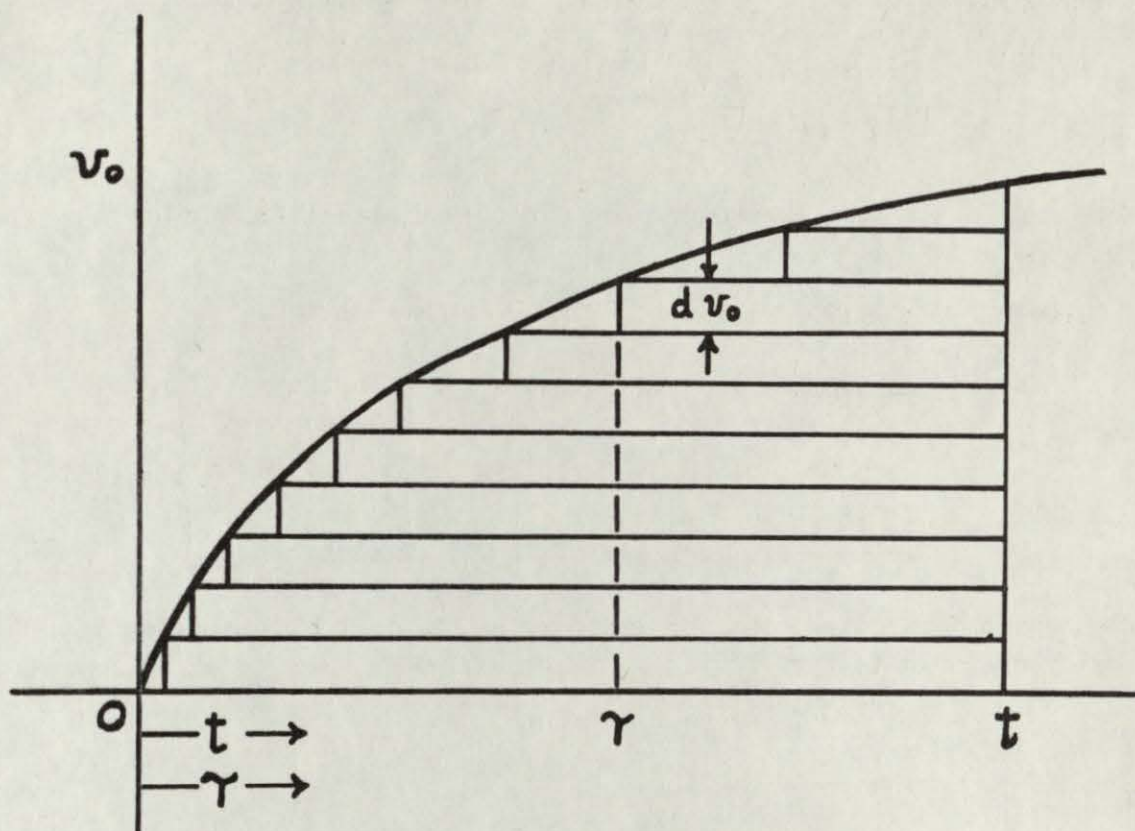


Fig. 25 Representation of a continuous velocity function $v_0(t)$ by a series of step functions.

Changing the integration variable from v_0 to τ , this becomes

$$s(x, t) = \int_0^t s_u[x, (t-\tau)] v_0'(\tau) d\tau, \quad (147)$$

where the prime indicates differentiation. Integrating by parts (147) becomes

$$s(x, t) = \left[s_u[x, (t-\tau)] v_0(\tau) \right]_0^t + \int_0^t \left(\frac{\partial s_u(x, t)}{\partial t} \right)_{t=t-\tau} v_0(\tau) d\tau \quad (148)$$

where in the integrand t is replaced by $(t-\tau)$ after the partial differentiation has been carried out. Since

$$s_u(x, 0) = 0, \text{ and } v_0(0) = 0 \quad (149)$$

the first term on the right hand side of (148) vanishes, leaving

$$s(x, t) = \int_0^t \left(\frac{\partial s_u(x, t)}{\partial t} \right)_{t=t-\tau} v_0(\tau) d\tau. \quad (150)$$

Here x is a constant parameter and t is held constant during the integration.

Referring to (88), (90), and Fig. 9, we see that

$$\left. \begin{aligned} \frac{\partial s_u(x, t)}{\partial t} &= 1 \quad \text{if } \frac{1}{c} (nL-x) < t < \frac{1}{c} (nL+x) \\ &\text{and } n = 1, 3, 5, 7, \dots ; \\ \frac{\partial s_u(x, t)}{\partial t} &= 0 \quad \text{for all other values of } t. \end{aligned} \right\} \quad (151)$$

Plotted as a function of t for fixed x , $\partial s_u(x, t)/\partial t$ appears graphically as shown in Fig. 26.

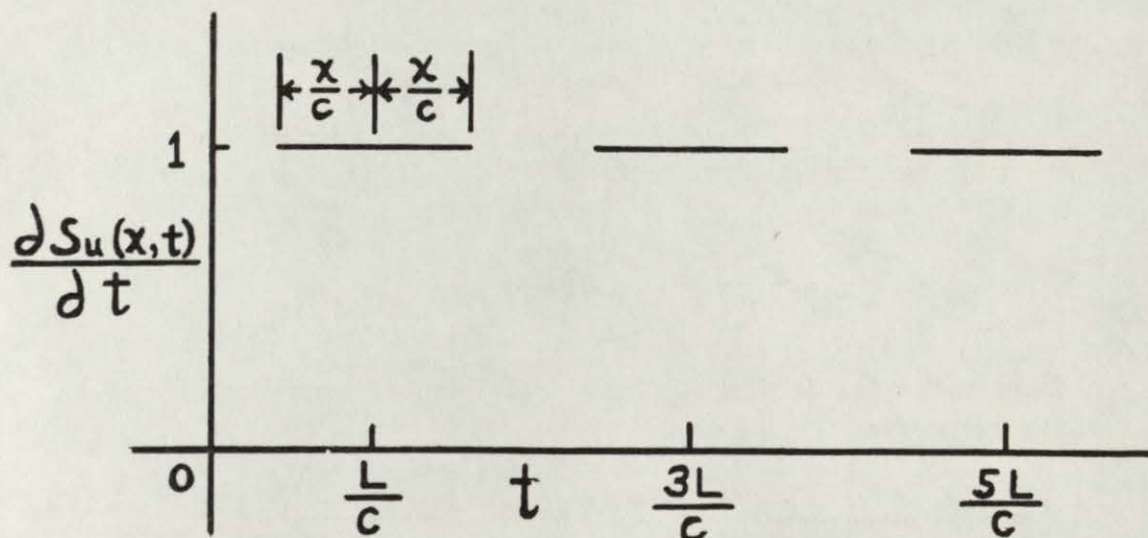


Fig. 26 Time derivative of the displacement due to an end velocity which is a unit step function.

Laying this off backward from time t we obtain a graph of $[\partial s_u(x,t)/\partial t]_{t=t-\tau}$. This and the other factor in the integrand of (150), namely, $v_0(\tau)$, are shown in Fig. 27. Since $s(x,t)$ is the integral of

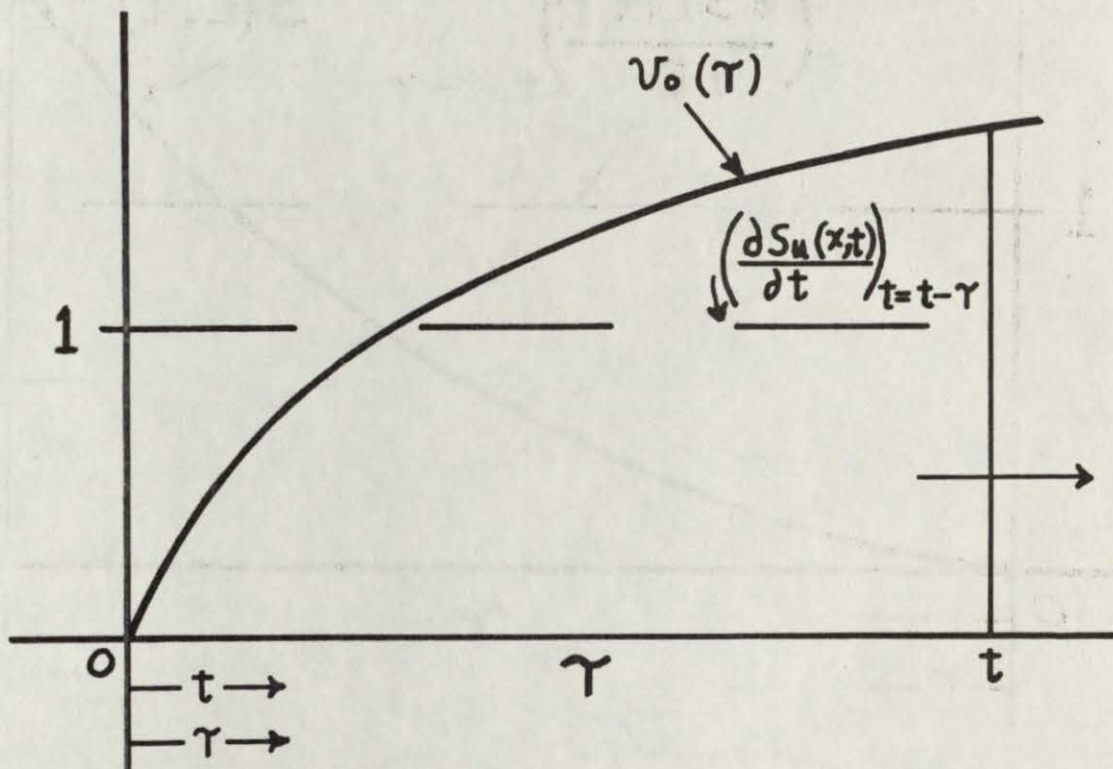


Fig. 27 Graph showing the two factors in the integrand of s , when the displacement is given by a superposition integral.

the product of the two factors we that $s(x,t)$ is given by the total area under those parts of the curve of $v_0(\tau)$ where the graph of the other factor $[\partial s_u(x,t)/\partial t]_{t=t-\tau}$ does not vanish. As t increases, this latter graph moves to the right, whereas the curve of $v_0(\tau)$ remains stationary. Since

$$\int_{\tau_1}^{\tau_2} v_0(\tau) d\tau = s(L, \tau_2) - s(L, \tau_1) = \Delta s(L, t) \quad (152)$$

we see that $s(x,t)$ is the sum of the increments of the end displacement curve $s(L, \tau)$ which occur over the intervals in which

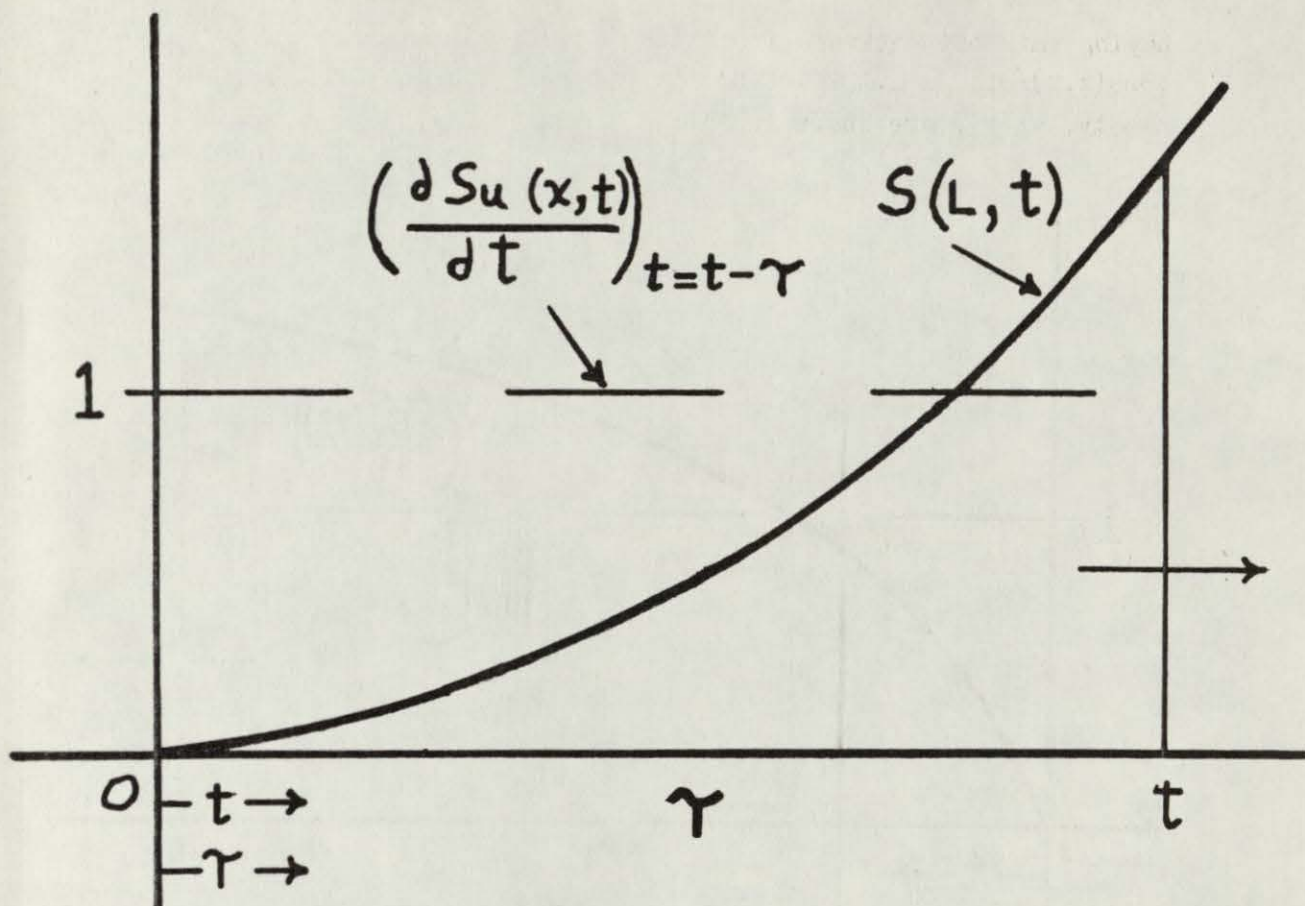


Fig. 28 Graphs of functions to be used in finding $s(x, t)$.

$\left[\frac{\partial s_u(x, t)}{\partial t} \right]_{t=t-\gamma}$ does not vanish, as indicated in Fig. 28. The end displacement curve $s(L, \tau)$ is, of course, given.

APPENDIX B

Calculation of the Numerical Approximation of the Motion of the Linear String When the Motion of the Moving End is Specified Arbitrarily.

Let us suppose that the displacements s_{ij}^* at the various lattice points involved in the approximate solution for the motion of the linear string when the moving end has a constant unit velocity are given. We wish to determine the displacements s_{ij} when the moving end has the arbitrarily specified motion s_{nj} . Placing

$$v_{nj} = \frac{1}{h} \Delta s_{nj} = n(s_{n,j+1} - s_{nj}) \quad j = 0, 1, 2, \dots \quad (153)$$

we see that the velocity in the $(j+1)^{\text{th}}$ time subinterval at the moving end, which is the $(j+1)^{\text{th}}$ subinterval in the right hand column of lattice points is v_{nj} , Fig. 29. As indicated in the figure,

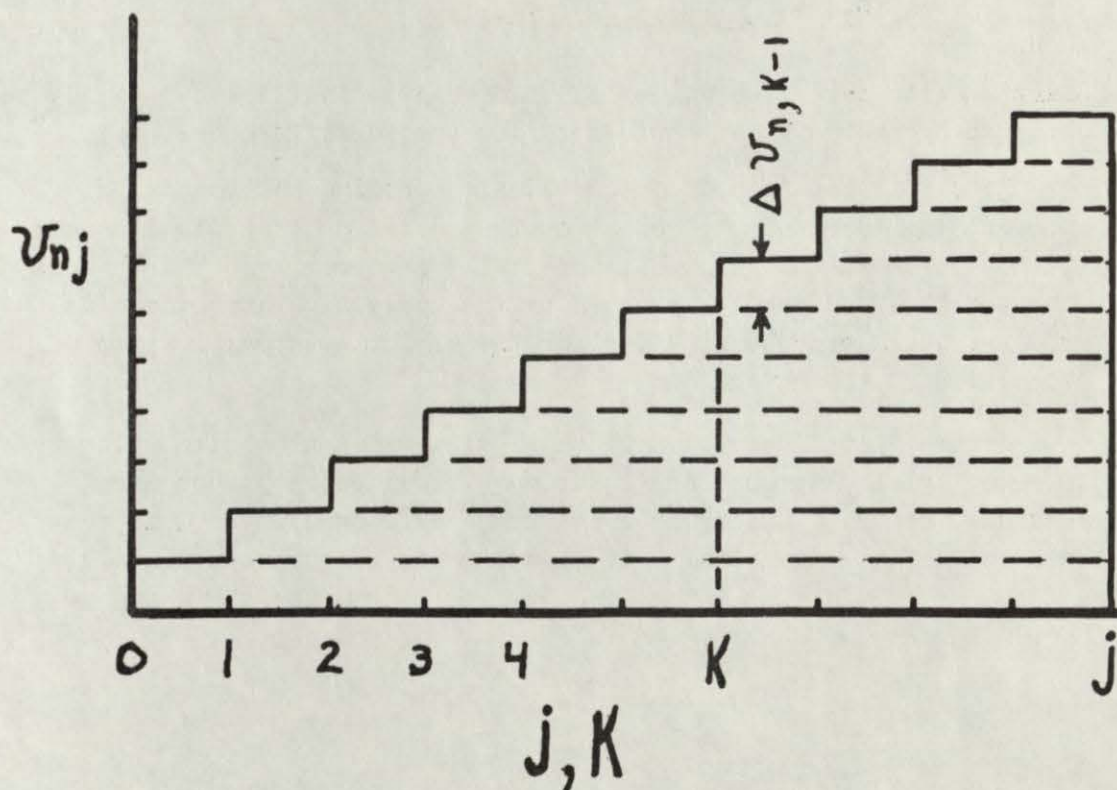


Fig. 29 Velocity of moving end of string. The actual velocity is approximated by adding a finite increment to v_n at each successive row.

the velocity of the moving end may be regarded to be composed of a number of abrupt increments which occur at different times, but continue indefinitely after they do occur. Placing

$$\Delta v_{nj} = v_{n,j+1} - v_{n,j} \quad (154)$$

we see that the increase in velocity at the time corresponding to the value k of the index is $\Delta v_{n,k-1}$.

Since the system is linear the displacement, s_{ij} may be regarded to be composed of the effects of the various velocity increments, these being superimposed. The contribution to s_{ij} of the velocity increment $\Delta v_{n,k-1}$ which occurs at k is

$$s_{i,j-k}^* \Delta v_{n,k-1} ; \quad (155)$$

hence adding these contributions we obtain finally

$$s_{ij} = \sum_{k=0}^{j-1} s_{i,j-k}^* \Delta v_{n,k-1} . \quad (156)$$

Starting with the given values of s_{nj} the Δv 's in (156) can easily be obtained by making a table of first and second differences.

If s_{ij}^* is obtained from the solution obtained by solving difference equations, then (156) gives the corresponding solution when the motion of the moving end is specified arbitrarily. This can be used to check the result obtained by the successive approximation process, which process provides for the arbitrary specification of the motion of the moving end.

If the specified motion of the moving end has no discontinuity in velocity, the approximate solution s_{ij} may be very much more accurate than s_{ij}^* , which involves such a discontinuity. This fact does not affect the validity of (156), which gives s_{ij} using s_{ij}^* .

REFERENCES

1. T. von Karman and P. Duwez, "The propagation of plastic deformation in solids", J. Appl. Phys. 21, 987-94 (1950).
2. G. I. Taylor, Scientific Papers of G. I. Taylor (Cambridge University Press, New York, 1958), Vol. 1, Paper No. 30, 456-63, and Paper No. 32, 467-79.
3. Kh. A. Rachmatulin, Prikl. Mat. i Mech. 9, 91-100 (1945).
4. M. N. Pilsworth, Jr. and H. J. Hoge, "Rate-dependent response of polymers to tensile impact", Textile Res. J. 35, 129-39 (1965).
5. M. N. Pilsworth, Jr., "Tensile impact on rubber and nylon", Quartermaster Research and Engineering Center, Natick, Mass. Tech. Rept. PR-3 (May 1962), 66 p.; AD-276525.
6. J. C. Smith and C. A. Fenstermaker, "Strain-wave propagation in strips of natural rubber subjected to high-velocity transverse impact", J. Appl. Phys. 38, 4218-24 (1967).
7. L. E. Malvern, "Plastic wave propagation in a bar of material exhibiting a strain rate effect", Quart. Appl. Math. 8, 405-11 (1951).
8. F. B. Hildebrand, Advanced Calculus for Applications (Prentice-Hall, 1964), p. 391.
9. P. D. Crout, Research Notebooks on Strain-Wave Propagation, No. 1, begun Sep. 1961, 152 p; No. 2, begun Sep. 1963, 152 p; and No. 3, begun Feb. 1967, 56 p. A set of these notebooks (Xerox copies of the originals) has been filed as an appendix to copy 1 of the present report, in the Technical Library of the U. S. Army Natick Laboratories.

DISTRIBUTION

Mr. Anthony L. Alesi
Army Materials and Mechanics
Research Center
Watertown, Mass. 02172

Prof. Stanley Backer
Textile Division
Dept. of Mechanical Engineering
Massachusetts Institute of Technology
Cambridge, Mass. 02139

Mr. F. G. Bocchetti
Dacron Research Laboratory Library
E. I. Dupont Co.
Kinston, North Carolina 28501

Prof. P. C. Chou
Drexel Institute of Technology
Philadelphia, Pa. 19104

Mr. R. E. Connell
Central Research Laboratory
Allied Chemical Corp.
Box 309
Morristown, N.J. 07960

Mr. Mark L. Dannis
Senior Research Associate
B. F. Goodrich Research Center
Brecksville, Ohio 44141

Mr. L. R. Easley
Bldg. 59
Tennessee Eastman Company
P. O. Box 511
Kingsport, Tenn. 37662

Mr. W. Julian Ferguson
Naval Research Laboratory
Washington, D. C. 20390

Prof. Francis B. Hildebrand
Mathematics Department
Massachusetts Institute of Technology
Cambridge, Mass. 02139

Dr. John D. Hoffman
Organic and Fibrous Materials
National Bureau of Standards
Washington, D. C. 20234

Prof. H. Kolsky
Brown University
Providence, Rhode Island 02912

Dr. A. M. Kotliar
Central Research Laboratory
Allied Chemical Corporation
Box 309
Morristown, N. J. 07960

Dr. Sudhir Kumar
U. S. Army Research Office, Durham
Box CM, Duke Station
Durham, North Carolina 27706

Prof. E. H. Lee
Applied Mechanics Department
Stanford University
Stanford, California 94305

Dr. W. James Lyons
Textile Research Institute
P. O. Box 625
Princeton, New Jersey 08540

Dr. Henry M. Morgan
Old Concord Road
Lincoln, Mass. 01773

DISTRIBUTION (cont'd)

Mr. Broham Norwick
Beaunit Textiles
450 Seventh Avenue
New York, N.Y. 10001

Plastics Technical Evaluation
Center
Attn: Harry E. Pebly, Jr., Chief
Picatinny Arsenal
Dover, New Jersey 07801

Mr. Jason Prumel
Central Research Laboratory
Allied Chemical Corp.
Box 309
Morristown, New Jersey 07960

Dr. Jack C. Smith
Institute for Materials Research
National Bureau of Standards
Washington, D. C. 20234

Mr. George M. Stewart
Biophysics Division
Army Chemical Center, Maryland 21401

Miss Judith Taylor
Rohm and Haas Company
Library, Box 219
Bristol, Pa. 19007

Dr. Guy Waddington, Director
Office of Critical Tables
National Academy of Sciences
2101 Constitution Avenue
Washington, D. C. 20418

Professor George P. Wadsworth
Mathematics Department
Massachusetts Institute of
Technology
Cambridge, Mass. 02139

Mr. Charles Warburton
Textile Research Institute
Princeton, New Jersey 08540

Dr. M. T. Watson
Bldg. 150
Tennessee Eastman Co.
P. O. Box 511
Kingsport, Tennessee 37662

Mr. Louis C. Weiss
Fiber Physics Investigations
U. S. Dept. of Agriculture
P. O. Box 19687
New Orleans, La. 70119

Dr. Anthony F. Wilde
Army Materials and Mechanics
Research Center
Watertown, Mass. 02172

Dr. Lawrence A. Wood
Institute for Materials Research
National Bureau of Standards
Washington, D. C. 20234

Unclassified

Security Classification

DOCUMENT CONTROL DATA - R & D

(Security classification of title, body of abstract and indexing annotation must be entered when the overall report is classified)

1. ORIGINATING ACTIVITY (Corporate author) U S. Army Natick Laboratories		2a. REPORT SECURITY CLASSIFICATION Unclassified	
		2b. GROUP	
3. REPORT TITLE RESPONSE OF POLYMERS TO TENSILE IMPACT. I. AN INTEGRAL-EQUATION, SUCCESSIVE-SUBSTITUTION SOLUTION FOR USE IN DIGITAL COMPUTERS, AND ITS APPLICATION TO A LINEAR ELASTIC MODEL.			
4. DESCRIPTIVE NOTES (Type of report and inclusive dates) 1st of 3 summarizing reports			
5. AUTHOR(S) (First name, middle initial, last name) Prescott D. Crout Malcolm N. Pilsworth, Jr. Harold J. Hoge			
6. REPORT DATE July 1968		7a. TOTAL NO. OF PAGES 71	7b. NO. OF REFS 9
8a. CONTRACT OR GRANT NO.		9a. ORIGINATOR'S REPORT NUMBER(S) 69-18-PR	
b. PROJECT NO. 1T061102B11A-07			
c.		9b. OTHER REPORT NO(S) (Any other numbers that may be assigned this report)	
d.			
10. DISTRIBUTION STATEMENT This document has been approved for public release and sale; its distribution is unlimited.			
11. SUPPLEMENTARY NOTES		12. SPONSORING MILITARY ACTIVITY U. S. Army Natick Laboratories Natick, Massachusetts	
13. ABSTRACT <p>An integral-equation, modified successive-substitution method of solving the equation of motion of a linear elastic string is derived. The method is an extension to two independent variables of a method previously employed with only a single independent variable. The solution is proved to be correct in the linear case and is expected to be valid also for nonlinear cases and for situations in which the response of the material is time dependent. Methods of numerical approximation based on a lattice of points in the time-position plane are developed, suitable for digital-computer programming. Typical results of computer runs on linear materials are presented.</p>			

DD FORM 1473
1 NOV 65REPLACES DD FORM 1473, 1 JAN 64, WHICH IS
OBSOLETE FOR ARMY USE.Unclassified
Security Classification

14. KEY WORDS	LINK A		LINK B		LINK C	
	ROLE	WT	ROLE	WT	ROLE	WT
Strains	8,9					
Strain rate	8,9					
Plastic deformation	8,9					
Tensile impact strength	8,9					
Strain propagation	8,9					
Polymers	9					
Polyamide resins	9					
Linear elastic material	9					
Numerical analysis	10					
Digital computers	10					
Stress Strain curves	10					
Successive substitution method	10					
Successive integration	10					